Behavioral/Cognitive

Neural Representation of Intraoral Olfactory and Gustatory Signals by the Mediodorsal Thalamus in Alert Rats

Kelly E. Fredericksen and Chad L. Samuelsen
Department of Anatomical Sciences and Neurobiology, University of Louisville, Louisville, Kentucky 40292

The mediodorsal thalamus is a multimodal region involved in a variety of cognitive behaviors, including olfactory attention, odor discrimination, and the hedonic perception of flavors. Although the mediodorsal thalamus forms connections with principal regions of the olfactory and gustatory networks, its role in processing olfactory and gustatory signals originating from the mouth remains unclear. Here, we recorded single-unit activity in the mediodorsal thalamus of behaving female rats during the intraoral delivery of individual odors, individual tastes, and odor-taste mixtures. Our results are the first to demonstrate that neurons in the mediodorsal thalamus dynamically encode chemosensory signals originating from the mouth. This chemoselective population is broadly tuned, exhibits excited and suppressed responses, and responds to odor-taste mixtures differently than an odor or taste alone. Furthermore, a subset of chemoselective neurons encodes the palatability-related features of tastes and may represent associations between previously experienced odor-taste pairs. Our results further demonstrate the multidimensionality of the mediodorsal thalamus and provide additional evidence of its involvement in processing chemosensory information important for ingestive behaviors.

Key words: **behavioral electrophysiology; flavor; mediodorsal thalamus; multimodal; odor; taste**

Significance Statement

The perception of food relies on the concurrent processing of olfactory and gustatory signals originating from the mouth. The mediodorsal thalamus is a higher-order thalamic nucleus involved in a variety of chemosensory-dependent behaviors and connects the olfactory and gustatory cortices with the prefrontal cortex. However, it is unknown how neurons in the mediodorsal thalamus process intraoral chemosensory signals. Using tetrode recordings in alert rats, our results are the first to show that neurons in the mediodorsal thalamus dynamically represent olfactory and gustatory signals from the mouth. Our findings are consistent with the mediodorsal thalamus being a key node between sensory and prefrontal cortical areas for processing chemosensory information underlying ingestive behavior.

Introduction

The perception of food, and ultimately the decision whether to eat it, requires the integration and discrimination of multisensory signals from the mouth (Sclafani, 2001; Verhagen and Engelen, 2006). While all senses contribute, concurrent activation of the olfactory and gustatory systems is essential for giving food its flavor (Small, 2012; Prescott, 2015). This multisensory process generates enduring odor-taste associations that are crucial for guiding future food choices (Fanselow and Birk, 1982; Schul et al., 1996; Sakai and Yamamoto, 2001; Gautam and Verhagen, 2010; Green et al., 2012; McQueen et al., 2020). These experience-dependent behaviors rely on a network of brain regions to integrate and process multimodal chemosensory signals to guide choice (Samuelsen and Vincis, 2021).

The thalamus receives inputs from various cortical and subcortical structures and is integral for communicating information across the brain (Roy et al., 2022). The thalamic subnuclei can be broadly divided into at least two categories: first-order and higher-order thalamic nuclei. First-order thalamic nuclei are primarily responsible for processing sensory input from the periphery and relaying it to the sensory cortex, whereas higher-order thalamic nuclei process and communicate information between cortical areas (Sherman, 2016; Nakajima and Halassa, 2017; Halassa and Sherman, 2019). The mediodorsal thalamus is a higher-order thalamic nucleus involved in an array of cognitive functions, including attention (Plailly et al., 2008; Veldhuizen and Small, 2011; Schmitt et al., 2017; Rikhye et al., 2018), valuation (Rousseaux et al., 1996; Sela et al., 2009; Tham et al., 2011; Alcaraz et al., 2018), memory (Parnaudeau et al., 2013; Bolkan et

Received Apr. 6, 2022; revised Sep. 14, 2022; accepted Sep. 21, 2022.

Author contributions: K.E.F. and C.L.S. designed research; K.E.F. performed research; K.E.F. and C.L.S. analyzed data; K.E.F. and C.L.S. wrote the first draft of the paper; K.E.F. and C.L.S. edited the paper; K.E.F. and C.L.S. wrote the paper.

This work was supported by the National Institute of Deafness and Other Communication Disorders Grant R01-DC018273 (to C.S.). We thank Dr. Roberto Vincis and Dr. Sanaya Stocke for the helpful comments and discussions.

The authors declare no competing financial interests.

Correspondence should be addressed to Chad L. Samuelsen at chad.samuelsen@louisville.edu.

https://doi.org/10.1523/JNEUROSCI.0674-22.2022

al., 2017; Scott et al., 2020), and stimulus-outcome associations (Oyoshi et al., 1996; Kawagoe et al., 2007; Courtiol and Wilson, 2016). It receives projections from primary olfactory cortical areas (e.g., piriform cortex), is reciprocally connected with the gustatory cortex, and forms dense reciprocal connections with prefrontal cortical areas important for decision-making (Price and Slotnick, 1983; Kuroda et al., 1992; Ray and Price, 1992; Shi and Cassell, 1998; Kuramoto et al., 2017; Pelzer et al., 2017). Given its robust connectivity with olfactory areas, studies have examined the role of the mediodorsal thalamus in various experience-dependent olfactory behaviors, including olfactory attention (Plailly et al., 2008; Small et al., 2008; Tham et al., 2009; Veldhuizen and Small, 2011), odor discrimination (Eichenbaum et al., 1980; Staubli et al., 1987; Courtiol and Wilson, 2016; Courtiol et al., 2019), and odor-reward associations (Kawagoe et al., 2007). It is implicated in the hedonic perception of odors and flavors, as people with mediodorsal thalamus lesions report decreased hedonic ratings for experienced odors and odor-taste mixtures (Tham et al., 2011). Electrophysiological experiments in anesthetized and behaving rats have shown that neurons in the mediodorsal thalamus encode odors sampled by sniffing (i.e., orthonasal olfaction; Courtiol and Wilson, 2014) and display odor selectivity during olfactory discrimination tasks (Courtiol and Wilson, 2016). However, it is unknown how mediodorsal thalamus neurons represent orally consumed odors, tastes, and odor-taste mixtures.

To address this question, we recorded single-unit activity in the mediodorsal thalamus of behaving rats during the intraoral delivery of three stimulus categories: individual odors, individual tastes, and odor-taste mixtures. This approach allowed odorized stimuli to be detected via retronasal olfaction, an essential factor for flavor perception (Verhagen and Engelen, 2006; Prescott, 2012). It also ensured that all chemosensory stimuli would share similar somatosensory and attentional attributes associated with the intraoral delivery of liquids. Our data provide novel insights into how the mediodorsal thalamus processes chemosensory signals originating from the mouth. Our findings demonstrate that mediodorsal thalamus neurons respond broadly across intraoral stimuli with time-varying multiphasic changes in activity. This chemoselective population reliably encodes unimodal and multimodal chemosensory signals over time, with a subpopulation representing the palatability-related features of tastes and associations between experienced odor-taste pairs. Our results are consistent with the mediodorsal thalamus being an integral component of the network processing of chemosensory signals by communicating information between sensory and prefrontal cortical areas important for ingestive behavior.

Materials and Methods

Experimental subjects

All procedures were performed in accordance with university, state, and federal regulations regarding research animals and were approved by the University of Louisville Institutional Animal Care and Use Committee. Female Long-Evans rats (~250–350 g, Charles Rivers) were single-housed and maintained on a 12/12 h light/dark cycle with *ad libitum* access to food and distilled water unless specified otherwise.

Surgery and tetrode implantation

Rats were anesthetized in an isoflurane gas anesthesia induction chamber with a 5% isoflurane/oxygen mix. Once sedated, rats were removed, and an isoflurane mask was placed on them. Rats received preoperative injections of buprenorphine HCl (0.05 mg/kg), atropine (0.03 mg/kg), dexamethasone (0.2 mg/kg), and lactated Ringers solution (5 ml). Once a surgical level of anesthesia was reached, the scalp was shaved, and the rat was placed into a stereotaxic frame. The depth of anesthesia was maintained with a 1.5–3.5% isoflurane/oxygen mix and monitored every 15 min by inspection of the breathing rate, whisking, and the toe-pinch withdrawal reflex. Ophthalmic ointment was placed on the eyes, and the scalp was swabbed with a povidone-iodine solution followed by a 70% ethanol solution. A midline incision was made, and the skull was cleaned with a 3% hydrogen peroxide solution. Cranial holes were drilled for the placement of seven anchoring screws (Microfasteners, SMPPS0002). A craniotomy was performed over the right mediodorsal thalamus (AP: −3.3 mm, ML: 1.4–1.6 mm from bregma) to implant a drivable bundle of eight tetrodes (Sandvik-Kanthal, PX000004) with a final impedance of ~200–300 kΩ. The medial and central portions of the mediodorsal thalamus were targeted because of their connectivity with olfactory and gustatory cortical areas (Price and Slotnick, 1983; Kuroda et al., 1992; Ray and Price, 1992; Shi and Cassell, 1998; Pelzer et al., 2017). The tetrode bundle was inserted at a 10° angle, to avoid the superior sagittal sinus, and to a depth of ~4.7 mm from the brain surface. Ground wires were secured to multiple anchoring screws. Intraoral cannulas (IOCs) were bilaterally inserted to allow for the delivery of solutions containing stimuli directly into the oral cavity. All implants and a head-bolt (for head restraint) were cemented to the skull with dental acrylic. Injections of analgesic (buprenorphine HCl) were provided for 2–3 d after surgery. Rats were allowed a recovery period of 7–10 d before beginning water restriction.

Stimulus delivery and recording procedure

Following recovery from surgery, rats began a water restriction regime where they received access to a bottle containing distilled water for 1 h each day in their home cage. Once acclimated to the water restriction regime, rats were given 1 h access in their home cage for four consecutive days to two bottles containing different odor-taste mixtures: a palatable mixture of 0.01% isoamyl acetate-100 mM sucrose and an unpalatable mixture of 0.01% benzaldehyde-200 mM citric acid. Experience with odor-taste mixtures generates associations between the quality and value of an odor and a taste (Fanselow and Birk, 1982; Holder, 1991; Stevenson et al., 1995; Prescott et al., 2004; Gautam and Verhagen, 2010; Green et al., 2012; McQueen et al., 2020), but it is unclear how many exposures to an odor-taste mixture are necessary to generate these associations. Therefore, we provided rats multiple days of exposure to odor-taste mixtures to establish odor-taste associations and limit possible variability across sessions related to learning odor-taste associations. Previous studies have shown that multiple days of exposure to odor-taste mixtures is sufficient to establish odor-taste associations (Sakai and Yamamoto, 2001; McQueen et al., 2020). This experience had the additional benefit of reducing the likelihood of rats rejecting odorized stimuli because of neophobia (Miller et al., 1986; Lin et al., 2009; Fredericksen et al., 2019; McQueen et al., 2020). After each recording session, rats were given 1-h access in their home cage to the two bottles containing the previously presented odor-taste mixtures to support experienced odor-taste associations throughout the experiment.

After odor-taste mixture experience, rats were trained to wait calmly in a head-restrained position for the intraoral delivery of liquids through the IOCs. All stimuli were mixed with distilled water and delivered via manifolds of polyimide tubes placed in the IOCs. Stimuli included distilled water [W], tastes (100 mM sucrose [S], 100 mM NaCl [Na], 200 mM citric acid [CA], and 1 mM quinine [Q]), odors (0.01% isoamyl acetate [IA], 0.01% benzaldehyde [B], and 0.01% methyl valerate [MV]), the previously experienced odor-taste mixtures (isoamyl acetate-sucrose [IA-S] and benzaldehyde-citric acid [B-CA]), and mismatched pairings of those mixtures (isoamyl acetate-citric acid [IA-CA] and benzaldehyde-sucrose [B-S]). These odors have been used in previous studies investigating orally consumed odors (Aimé et al., 2007; Julliard et al., 2007; Gautam and Verhagen, 2010, 2012; Tong et al., 2011; Rebello et al., 2015; Samuelsen and Fontanini, 2017; Bamji-Stocke et al., 2018; Fredericksen et al., 2019; McQueen et al., 2020). At these concentrations, isoamyl acetate and benzaldehyde lack a gustatory component (Aimé et al., 2007; Gautam and Verhagen, 2010; Samuelsen and Fontanini, 2017). A trial began with an intertrial interval of 20 ± 5 s followed by the

pseudo-random delivery of ~25–30 µl (pressure infused via computer-controlled solenoid valves, opening time ~25 ms) of water, a single taste, a single odor, or an odor-taste mixture. Each stimulus delivery was followed 5 s later by a ~40-µl distilled water rinse. Although intraoral delivery directly infuses chemosensory stimuli into the oral cavity, rats can still reject stimuli by not swallowing and allowing fluids to leak from the mouth. If a rat failed to consume an intraoral stimulus, the session was immediately aborted. Only trials where rats consumed all 12 stimuli were included in the analysis. All recording sessions consisted of 120 trials (i.e., 12 stimuli × 10 trials), except for one session where a rat received only nine trials per stimulus. Tetrode bundles were lowered ~160 µm further after each recording session to obtain a new ensemble of neurons.

Electrophysiological recordings

Signals were sampled at 40 kHz, digitized, and bandpass filtered using the Plexon OmniPlex D system (Plexon, RRID:SCR_014803). Single units were isolated offline using a combination of template algorithms, cluster-cutting, and examination of interspike-interval plots using Offline Sorter (Plexon, Offline Sorter; RRID:SCR_000012). Single units were required to have interspike intervals longer than the biological constraints of a neuronal refractory period (>1 ms; 0% refractory period violations). Data analysis was performed using Neuroexplorer (Nex Technologies; RRID:SCR_001818) and custom-written scripts in MATLAB (The MathWorks, RRID:SCR_001622).

Analysis of single units

For each neuron, single-trial activity and peristimulus time histograms (PSTHs) were aligned to the stimulus presentation through the IOCs. Responses to chemosensory stimuli were evaluated by analyzing changes in firing rates (FR) as in previous studies (Samuelsen et al., 2013; Jezzini et al., 2013; Gardner and Fontanini, 2014; Liu and Fontanini, 2015; Samuelsen and Fontanini, 2017; Levitan et al., 2019; Bouaichi and Vincis, 2020). Neurons were defined as "chemoselective" when two criteria were satisfied: (1) stimulus-evoked activity significantly differed from baseline for at least one stimulus and (2) there was a significant difference in the activity evoked by the twelve intraoral stimuli. A one-sample Kolmogorov–Smirnov test found that the spiking activity of neurons in the mediodorsal thalamus were not normally distributed. Therefore, significant difference from baseline for each stimulus was established using a nonparametric Wilcoxon rank-sum comparison between a 2 s baseline window (binned in 200-ms increments; 10-trial × 10-bin, concatenated into 100 × 1 baseline-array) immediately before stimulus delivery (i.e., baseline) and each 200-ms bin (10-trial × 1-bin array) following stimulus delivery (5 s poststimulus) with correction for family-wise error (two consecutive significant bins, $p < 0.05$; Gardner and Fontanini, 2014; Samuelsen and Fontanini, 2017; Bouaichi and Vincis, 2020).

Since a nonparametric statistic is not available to determine significant interactions between chemosensory-evoked activity and time, a two-way ANOVAs (stimulus × time; Samuelsen et al., 2013; Jezzini et al., 2013; Gardner and Fontanini, 2014; Liu and Fontanini, 2015; Samuelsen and Fontanini, 2017; Levitan et al., 2019; Bouaichi and Vincis, 2020) was used to determine differences in the magnitude and time course of the chemosensory-evoked activity across the 12 stimuli (200-ms bins from 0 to 5 s after stimulus delivery) with a conservative α ($p < 0.01$). A neuron was considered to respond differently among the intraoral stimuli when the stimulus main effect or the interaction term (stimulus × time) had a value of $p < 0.01$ (see extended data table in Extended Data Table 2-1 for the results of two-way ANOVAs for each of the 85 chemoselective neurons). The distribution of responses and tuning of the chemoselective population were compared using a χ^2 test ($p < 0.05$) with *post hoc* comparisons performed using Fisher's exact test with Dunn–Sidak correction for family-wise error (Shan and Gerstenberger, 2017).

Area under the receiver operating characteristic (auROC) normalization method

To avoid potential confounds introduced by differences in baseline and evoked firing rates among neurons, stimulus-evoked activity was normalized to its baseline activity using the auROC method when comparing responses by groups of neurons (Cohen et al., 2012; Jezzini et al., 2013; Gardner and Fontanini, 2014; Liu and Fontanini, 2015; Vincis and Fontanini, 2016; Samuelsen and Fontanini, 2017; Bouaichi and Vincis, 2020). This method normalizes each neuron's stimulus-evoked activity to baseline activity using a scale of 0–1, where 0.5 represents the median of equivalence of the baseline activity. The auROC values represent the probability that the spike counts during each 200-ms bin is significantly greater than the spike counts during the baseline period (−2–0 s). A score of 1 indicates that all values in the tested bin are greater than baseline, whereas a score of 0 indicates that all values are less than baseline. Therefore, a value >0.5 indicates an excited response and a value <0.5 indicates a suppressed response. Population PSTHs were generated by averaging the auROC-normalized response to a given stimulus for each neuron in the observed population. Comparisons of the auROC-normalized population activity were performed using the Friedman test ($p < 0.05$).

Excited and suppressed responses

To determine whether a chemoselective neuron exhibited an excited or a suppressed response to an intraoral stimulus, we calculated the mean auROC value of all bins that significantly differed from baseline. Responses with an average significant auROC value >0.5 were defined as excited, and those with an average significant auROC value <0.5 were defined as suppressed. Comparisons in the time course between nonresponses and responses that were excited or suppressed by chemosensory stimuli were performed using the Wilcoxon rank-sum test with correction for family-wise error (two consecutive significant bins, $p < 0.05$). Heat maps were generated that show all significant responses to each stimulus plotted from the lowest average significant auROC value (suppressed) to the greatest average significant auROC value (excited). The period during which a significant difference from baseline occurred was determined using a sliding window of 100 ms, stepped in 20-ms increments, until the firing rate was 2.58 SDs (99% confidence level) above or below the average baseline firing rate (2 s before stimulus delivery; Bouaichi and Vincis, 2020). The response latency (i.e., time from stimulus delivery to first significant difference from baseline) was recorded as the trailing edge of the first significant bin. The response duration (i.e., total amount of time significantly different from baseline) was calculated as the total number of 20-ms bins significantly above (excited) or below (suppressed) the average baseline firing rate. Differences in response latency and response duration between excited and suppressed responses were compared using a two-sample Kolmogorov–Smirnov test ($p < 0.05$). Comparisons of response latency and response duration between stimulus categories were performed using the Kruskal–Wallis test corrected with the Tukey's HSD test ($p < 0.05$).

Population decoding analysis

Population decoding analyses were performed using an open source pattern classifier algorithm (for a detailed description of the Neural Decoding Toolbox, see Meyers, 2013). This analysis uses the pattern of firing rates of a population of neurons to make predictions about which stimulus was delivered during a given trial. The accuracy of the classifier indicates how the population of neurons in the mediodorsal thalamus represents intraoral stimuli and how that chemosensory information is processed over time. For each subpopulation of neurons, a firing rate matrix of the spike times of each neuron (2 s before to 5 s after stimulus delivery) was realigned to the stimulus delivery, compiled into 250-ms bins, and normalized to the Z score. Four firing rate matrices were constructed for each subpopulation: (1) all 12 stimuli, (2) water and the three odors, (3) water and the four tastes, and (4) water and the four odor-taste mixtures. Water was included in each category as a general nonchemosensory stimulus. Matrix activity was divided into nine sets: eight "training sets" were used by the classifier algorithm to "learn" the relationship between the population's neural activity pattern and the different stimuli; one "testing set" was used to predict which stimulus was delivered given the population's pattern of activity that was used to train the classifier. A max correlation coefficient classifier was used to assess

stimulus-related information represented by the population activity. The max correlation coefficient classifier calculates the correlation coefficient between a test trial and each of the training set stimulus templates; the stimulus template with the largest correlation coefficient value is selected as the predicted stimulus. To compute the classification accuracy, this process was repeated ten times using different testing and training sets each time. The classification accuracy was defined as the fraction of trials during each bin for which the classifier correctly predicted the stimulus. Comparisons of the classification accuracy between neuron populations were performed using a permutation test ($p < 0.05$; Ojala and Garriga, 2010).

A confusion matrix is a visual representation of the decoding performance for each stimulus, where columns represent the actual stimulus and rows represent the predicted stimulus. White squares represent classification accuracy less than chance, and darker hues indicate better performance. Diagonal squares represent the proportion of trials in which the classifier correctly assigned the predicted stimulus to its true stimulus. Squares outside the diagonal represent the predicted stimuli that the classifier most often "confused" for each true stimulus (i.e., false predictions). Comparisons between populations of neurons in the proportion of trials where the predicted stimulus did not match the true stimulus were made with the Wilcoxon rank-sum test ($p < 0.05$). The Kruskal–Wallis test with Tukey's HSD correction for family-wise error ($p < 0.05$) was used to determine whether the classifier was more likely to confuse different groups of stimuli with each other.

Mixture-component difference (MCD) analysis

The MCD is equal to the difference in firing rate (−2–5 s; 200-ms bins) between the response to an odor-taste mixture (e.g., isoamyl acetate-sucrose) and the response to the odor component alone (e.g., isoamyl acetate) or the taste component alone (e.g., sucrose). A positive MCD score indicated that the mixture-evoked activity was higher than the component-evoked activity, while a negative MCD score indicated that the component-evoked activity was higher than the mixture-evoked activity. This analysis was used to examine eight mixture-stimulus differences (four mixture-odor and four mixture-taste) for each chemoselective neuron ($n = 85$) for a total of 680 mixture-component difference responses. Unlike the activity evoked by intraoral stimulus delivery, baseline activity is not directly related to an event. This variability in baseline activity can artificially enhance individual baseline MCD scores. To mitigate this variability, we calculated the mean and SD using the baseline MCD scores of the eight mixture-stimulus differences for each chemoselective neuron. A response was considered significant when an evoked MCD score exceeded the mean of the eight baseline MCD scores ± six times the SD. The absolute difference in the MCD value was used to calculate the average MCD time course to account for the differences between mixtures and components regardless of whether the mixture or the component had the greater firing rate. Significant changes from baseline in the average MCD time course were determined using a Wilcoxon rank-sum test with correction for family-wise error (two consecutive significant bins, $p < 0.05$).

Palatability index (PI) analysis

A PI was used to evaluate whether the activity of neurons in the mediodorsal thalamus represents the palatability-related features of tastes (Fontanini et al., 2009; Piette et al., 2012; Jezzini et al., 2013; Liu and Fontanini, 2015; Samuelsen and Fontanini, 2017; Bouaichi and Vincis, 2020). This analysis quantified differences in activity between tastes with similar hedonic values (sucrose/NaCl, citric acid/quinine) and tastes with opposite hedonic values (sucrose/quinine, sucrose/citric acid, NaCl/quinine, NaCl/citric acid). To control for differences in firing rates across the population of chemoselective neurons, the auROC-normalized activity (–2–5 s, 200-ms bins) was used to estimate the differences between taste pairs. The PI score was defined as the difference in the absolute value of the log-likelihood ratio of the auROC-normalized firing rate for taste responses with opposite ($<|LR|>_{opposite}$) and similar ($<|LR|>_{same}$) hedonic values. The PI was defined as follows: ($<|LR|>_{opposite} - <|LR|>_{same}$), where:

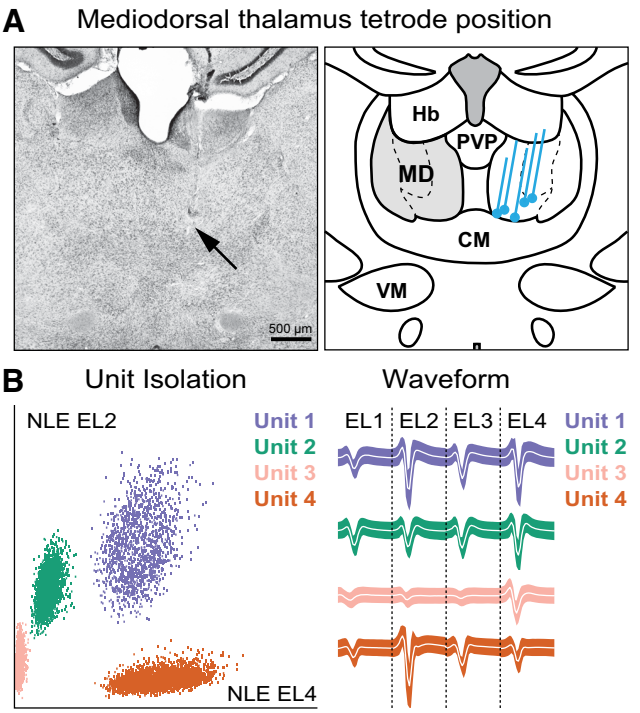

Figure 1. Tetrode locations and representative single-unit recordings. ***A***, Left, Example histologic section showing the recording tetrode position (black arrow) in the mediodorsal thalamus. Right, Schematic summary of the reconstructed tetrode path in five rats. The blue lines correspond to the dorsoventral range of each drivable tetrode bundle. CM, central medial thalamic nucleus; Hb, habenular nucleus; MD, mediodorsal thalamus; PVP, paraventricular thalamic nucleus; VM, ventromedial thalamic nucleus. ***B***, Left, Representative single-unit recordings in the mediodorsal thalamus showing the principal component analysis of waveform shapes of four individual neurons. EL, electrode; NLE, nonlinear energy. Right, Average single-unit response for the same four neurons recorded from the four wires of the tetrode.

$$<|LR|>_{same} = 0.5 \times \left(\left| \ln \frac{\text{sucrose}}{\text{NaCl}} \right| + \left| \ln \frac{\text{quinine}}{\text{citric acid}} \right| \right)$$

$$<|LR|>_{opposite} = 0.25 \times \left(\left| \ln \frac{\text{sucrose}}{\text{quinine}} \right| + \left| \ln \frac{\text{sucrose}}{\text{citric acid}} \right| + \left| \ln \frac{\text{NaCl}}{\text{quinine}} \right| + \left| \ln \frac{\text{NaCl}}{\text{citric acid}} \right| \right)$$

A positive PI score indicates that a neuron responds similarly to tastes with similar palatability and differently to stimuli with opposite palatability. A chemoselective neuron was deemed palatability-related when the evoked PI score was positive and exceeded the mean ± six times the SD of the baseline (Bouaichi and Vincis, 2020). Significant changes from baseline in the average PI score time course were determined using a Wilcoxon rank-sum test with correction for family-wise error (two consecutive significant bins, $p < 0.05$).

Histology

After recordings were completed, rats were anesthetized with a ketamine/xylazine/acepromazine mixture (100, 5.2, and 1 mg/kg), and DC current (7 µA for 7 s) was applied to mark the tetrode locations. Rats were then transcardially perfused with cold phosphate buffer solution followed by 4% paraformaldehyde (PFA). Brains were extracted, post-fixed in 4% PFA, and then incubated in 30% sucrose. Sections were cut 70 µm thick using a cryostat, mounted, and stained with cresyl violet. Tetrode placement within the mediodorsal thalamus was required for recording sessions to be included in the data analysis (Fig. 1).

Experimental design and statistical analysis

As with previous head-fixed recording experiments (Jones et al., 2007; Fontanini et al., 2009; Samuelsen et al., 2012, 2013; Gardner and

Fontanini, 2014; Vincis and Fontanini, 2016; Samuelsen and Fontanini, 2017), only adult female rats were used because the size and strength of adult male rats significantly increases the risk of catastrophic head-cap failure. All chemosensory stimuli were delivered pseudo-randomly according to custom-written MATLAB (The MathWorks) scripts. Experimenters had no control over the order of stimulus delivery. All statistical analyses were performed using GraphPad Prism (GraphPad Software) and MATLAB (The MathWorks), including population decoding analyses using the Neural Decoding Toolbox (Meyers, 2013). No statistical methods were used to predetermine sample sizes, but the numbers of recorded neurons and animals in this study are similar to those reported in previous studies.

Results

Previous electrophysiological studies have shown that neurons in the mediodorsal thalamus represent the identity of odors sampled via orthonasal olfaction (Yarita et al., 1980; Imamura et al., 1984; Courtiol and Wilson, 2014, 2016), but it is unclear how chemosensory signals originating from the mouth are processed by the mediodorsal thalamus. To this aim, we recorded single-unit activity in the mediodorsal thalamus of behaving rats during the intraoral delivery of distilled water, individual odors, individual tastes, and odor-taste mixtures. Figure 1 shows a representative example and a schematic illustration of the dorsal-ventral range of recording electrodes in the mediodorsal thalamus of each animal. A total of 135 single neurons were recorded from five rats across 27 sessions (5.4 ± 0.4 sessions per rat) with an average yield of 5.1 ± 0.9 neurons per session.

Neurons in the mediodorsal thalamus represent intraoral chemosensory signals

As a first step in evaluating chemosensory processing by the mediodorsal thalamus, we identified the population of neurons that responded differently to various odors, tastes, and odor-taste mixtures (i.e., chemoselective). Neurons defined as "chemoselective" exhibited a significant change in activity compared with baseline for at least one stimulus and responded differently across the various intraoral stimuli (see Materials and Methods for details). These two criteria were purposefully stringent because the intraoral delivery of solutions could introduce potential confounds related to the general effects of somatosensation or attention rather than chemosensory-related activity. We found that 63% (85/135) of the neurons recorded from the mediodorsal thalamus met both criteria, and therefore we focused our analyses on this chemoselective population.

To better understand how intraoral chemosensory signals are processed by the mediodorsal thalamus, we analyzed the responses of the chemoselective population to odors, tastes, and odor-taste-mixtures (Fig. 2). Visual inspection of representative neurons and the average responses of the chemoselective population to water and the three odors (Fig. 2*A*), the four tastes (Fig. 2*B*), and the four odor-taste mixtures (Fig. 2*C*) suggested that responses differed between the chemosensory stimuli categories (i.e., odors, tastes, and odor-taste mixtures). A comparison of the auROC-normalized population activity showed an overall difference in the responses evoked by the 12 intraoral stimuli (Freidman's test, $\chi^2_{11} = 58.28$, $p < 0.001$). Therefore, we next sought to determine whether the population responses differed within the three chemosensory stimuli categories. Although there was no significant difference in the responses to the three odors (Fig. 2*A*, Freidman's test, $\chi^2_2 = 2.02$, $p = 0.364$), the chemoselective population's responses differed across the four tastes (Fig. 2*B*, Freidman's test, $\chi^2_3 = 31.08$, $p < 0.001$) and the four odor-taste mixtures (Fig. 2*C*, Freidman's test, $\chi^2_3 = 15.12$, $p = 0.002$).

Next, we examined whether different proportions of chemoselective neurons responded to the various intraoral stimuli. Figure 2*D–F* shows the distribution of neurons that responded to water and each of the three odors (Fig. 2*D*), the four tastes (Fig. 2*E*), and the four odor-taste mixtures (Fig. 2*F*). There was an overall significant difference in the proportion of neurons responding to the various intraoral stimuli ($\chi^2_{11} = 56.99$, $p < 0.001$), with the majority of chemoselective neurons (60.0%, 51/85) responding to stimuli from all three categories. Analysis of the response distribution within each chemosensory category showed no difference in the proportion of neurons responding to the different odors (Fig. 2*D*, $\chi^2_2 = 0.028$, $p = 0.986$) or odor-taste mixtures (Fig. 2*F*, $\chi^2_3 = 2.477$, $p = 0.480$) but showed a significant difference among the taste stimuli (Fig. 2*E*, $\chi^2_3 = 22.38$, $p < 0.001$). *Post hoc* analyses showed that significantly more neurons responded to citric acid (65.9%, 56/85) than responded to sucrose (38.8%, 33/85; Fisher's exact test, $p < 0.001$) or salt (31.7%, 27/85; Fisher's exact test, $p < 0.001$) but not quinine (48.2%, 41/85; Fisher's exact test, $p > 0.05$). More chemoselective neurons responded to the unpalatable citric acid than responded to either palatable taste.

Next, we evaluated the tuning profiles of chemoselective neurons within each stimulus category to determine the proportion of neurons that responded to only a single stimulus (i.e., sparsely tuned) or multiple stimuli (i.e., broadly tuned). Overall, most chemoselective neurons responded to at least one odor-taste mixture (92.9%, 79/85), followed by at least one taste (82.4%, 70/85), and then at least one odor (71.8%, 61/85). Within the odor category (Fig. 2*G*), there was no difference in the proportion of chemoselective neurons that did not respond to odors (28.2%, 24/85), responded to a single odor (31.8%, 27/85), or responded to multiple odors (40.0%, 34/85; $\chi^2(2) = 2.788$, $p = 0.25$). Within the taste category (Fig. 2*H*), the proportion of chemoselective neurons that responded to multiple taste stimuli ($\chi^2_2 = 29.36$, $p < 0.0001$, 55.3%, 47/85) was significantly greater than the proportion that responded to only a single taste (27.1%, 23/85; Fisher's exact test, $p < 0.001$) or did not respond to tastes (17.6%, 15/85; Fisher's exact test, $p < 0.001$). Within the odor-taste mixture category (Fig. 2*I*), the proportion of chemoselective neurons that responded to multiple odor-taste mixtures ($\chi^2_2 = 114.0$, $p < 0.001$, 77.6%, 66/85) was significantly greater than the proportion that responded to only a single odor-taste mixture (15.3%, 13/85; Fisher's exact test, $p < 0.001$) or did not respond to mixtures (7.1%, 6/85; Fisher's exact test, $p < 0.001$). For all three chemosensory categories, there was no difference in the proportions of neurons that responded to only one, only two, only three, or all four stimuli (Table 1; odors: $\chi^2_2 = 4.439$, $p = 0.11$; tastes: $\chi^2_3 = 6.116$, $p = 0.11$; mixtures: $\chi^2_3 = 5.128$, $p = 0.16$). These analyses showed that chemoselective neurons in the mediodorsal thalamus respond broadly across tastes and odor-taste mixtures but include a similar proportion of sparsely tuned and broadly tuned neurons responding to intraoral odors.

These analyses revealed that most neurons in the mediodorsal thalamus respond to the intraoral delivery of chemosensory stimuli, are primarily broadly tuned within chemosensory categories, and respond differently to unimodal and multimodal chemosensory signals. These results are consistent with neurons in the mediodorsal thalamus processing sensory information across a range of chemosensory stimuli.

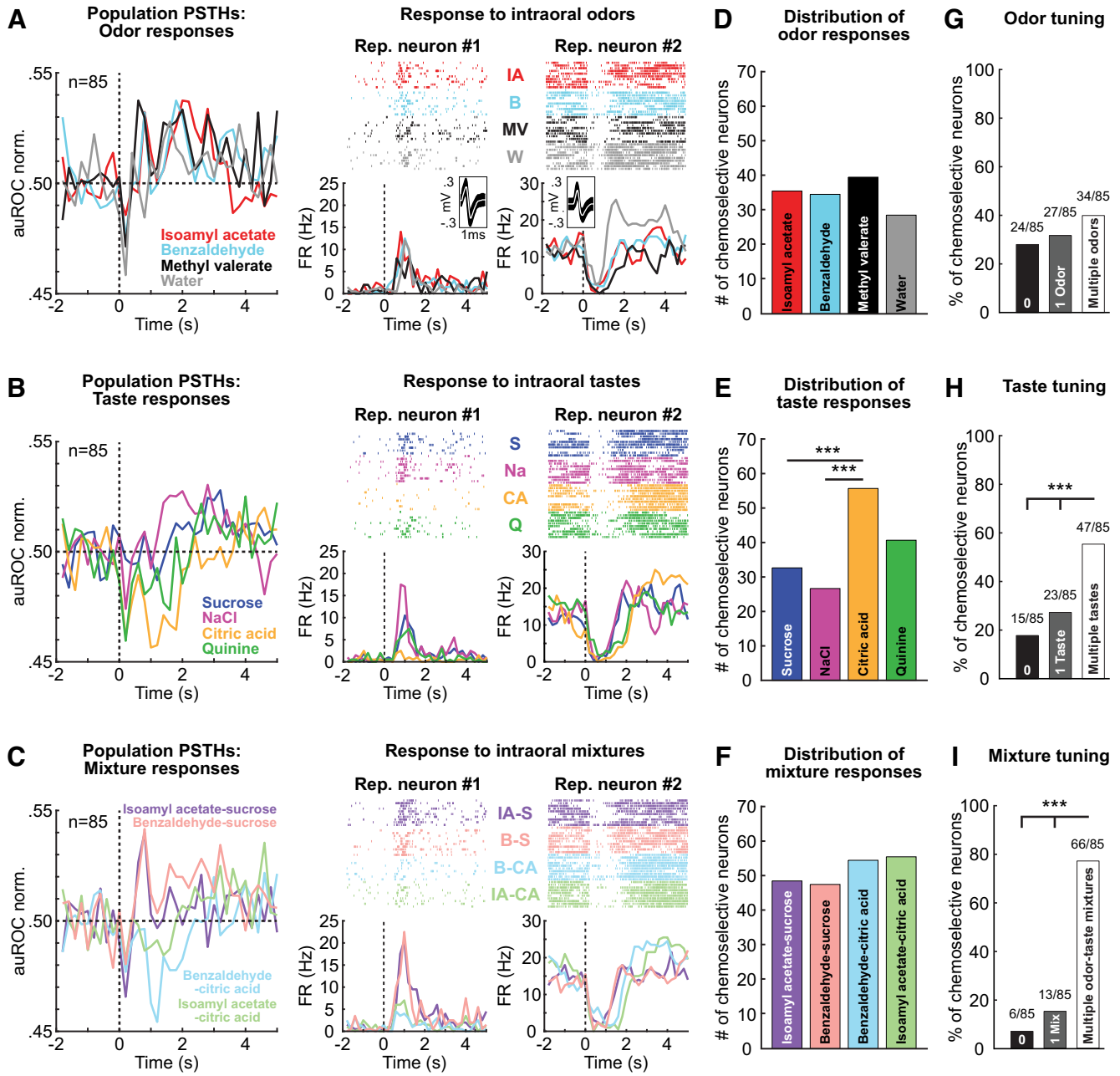

Figure 2. Neurons in the mediodorsal thalamus represent chemosensory signals originating in the mouth. ***A–C***, Left, Peristimulus time histograms (PSTHs) of the chemoselective population's ($n = 85$) normalized response (area under the receiver-operating characteristic curve; auROC-norm.) to (***A***) odors, (***B***) tastes, and (***C***) odor-taste mixtures. Vertical dashed lines indicate the stimulus delivery (time = 0). Horizontal dashed lines indicate baseline. The extended data table (Extended Data Table 2-1) shows the results of the two-way ANOVA test for each of the 85 chemoselective neurons. Right, Representative chemoselective neurons firing rate raster plots and PSTHs in response to intraoral delivery (time = 0, vertical dashed lines) of (***A***) water and the three odors [isoamyl acetate (IA; red), benzaldehyde (B; cyan), methyl valerate (MV; black), water (W; gray)], (***B***) the four tastes [sucrose (S; blue), NaCl (Na; magenta), citric acid (CA; yellow), quinine (Q; green)], and (***C***) the four odor-taste mixtures [isoamyl acetate-sucrose (IA-S; purple), benzaldehyde-sucrose (B-S; peach), benzaldehyde-citric acid (B-CA; light blue), isoamyl acetate-citric acid (IA-CA; light green)]. Insets, Average action potential waveforms for each neuron. ***D–F***, Distribution of the number of chemoselective neurons responding to (***D***) water and the three odors, (***E***) the four tastes, and (***F***) the four odor-taste mixtures. ***G–I***, Tuning profiles within each stimulus category show the proportion of chemoselective neurons that did not respond, responded to a single stimulus, or responded to multiple stimuli for (***G***) odors, (***H***) tastes, and (***I***) odor-taste mixtures; $^{***}p < 0.001$.

Table 1. Proportion of neurons responding to only one, two, three, or all four stimuli

	Only 1	Only 2	Only 3	All 4
Odors	27/85 (31.8%)	18/85 (21.2%)	16/85 (18.8%)	–
Tastes	23/85 (27.1%)	21/85 (24.7%)	12/85 (14.1%)	14/85 (16.5%)
Odor-taste mixtures	13/85 (15.3%)	26/85 (30.6%)	17/85 (20.0%)	23/85 (27.1%)

Temporal processing of chemosensory signals by the mediodorsal thalamus

Chemosensory processing in the olfactory and gustatory system is characterized by dynamic and time-varying modulations in activity (Katz et al., 2001; Fontanini et al., 2009; Maier et al., 2012; Samuelsen et al., 2012, 2013; Liu and Fontanini, 2015; Maier, 2017; Samuelsen and Fontanini, 2017). Although these areas primarily respond to chemosensory stimuli with excitation, a study by Liu and Fontanini (2015) examining another

thalamic nucleus, the gustatory thalamus (i.e., the parvicellular portion of the ventroposteromedial nucleus), revealed a near balance between taste-evoked excitation and suppression. Visual inspection of raster plots and PSTHs (Fig. 2*A–C*) indicated that chemoselective neuron activity could be excited or suppressed by the intraoral delivery of chemosensory stimuli. To evaluate responses by the chemoselective neuron population, we sorted chemosensory-evoked activity into excited responses (when the significant evoked activity was greater than baseline), suppressed responses (when the significant evoked activity was less than baseline), and nonresponses (activity that did not significantly differ from baseline). The auROC-normalized population averages of nonresponses, excited responses, and suppressed responses (Fig. 3*A–C*) and the heat maps of each significant response (Fig. 3*D–F*) to odors, tastes, and odor-taste mixtures illustrate the heterogeneity of responses across the chemoselective population. There was no significant difference in the overall proportion of responses that were excited (27.2%, 254/935) or suppressed (23.7%, 222/935) by the different chemosensory stimuli (Fisher's exact test, $p = 0.0998$). This equivalence in stimulus-evoked excitation and suppression was represented within each stimulus category. There was no difference in the proportion of odors that evoked excitation (23.5%, 60/255) or suppression (20.0%, 51/255; Fisher's exact test, $p = 0.391$), tastes that evoked excitation (24.1%, 82/340) or suppression (22.1%, 75/340; Fisher's exact test, $p = 0.585$), or odor-taste mixtures that evoked excitation (32.9%, 112/340) or suppression (28.2%, 96/340; Fisher's exact test, $p = 0.212$). Overall, chemosensory-evoked activity in the mediodorsal thalamus was balanced between excitation and suppression.

To determine whether temporal differences existed between excited and suppressed activity, we determined the response latency (i.e., time from stimulus delivery to first significant difference from baseline) and response duration (i.e., total amount of time the response was significantly different from baseline) for all chemosensory-evoked responses. Overall, responses suppressed by chemosensory stimuli (301.7 ± 30.1 ms) occurred significantly faster than those excited by chemosensory stimuli (443.9 ± 45.0 ms; two-sample Kolmogorov–Smirnov test, K-S stat = 0.23, $p < 0.001$). Next, we determined whether differences in response latency between excitation and suppression occurred across the chemosensory categories. While there was no difference among the stimulus categories in the response latency of excited activity (odors: 443.4 ± 82.8 ms, tastes: 471.6 ± 90.3 ms, odor-taste mixtures: 426.0 ± 65.5 ms; Kruskal–Wallis, $H(2) = 0.1080$, $p = 0.948$), this analysis revealed a significant difference among the stimulus categories for the response latency of suppression (Kruskal–Wallis, $H(2) = 8.9704$, $p = 0.011$). Tukey's HSD test for multiple comparisons showed that the response latency of suppression occurred significantly faster with the intraoral delivery of odor stimuli (156.1 ± 36.1 ms) than that for either taste (341.0 ± 55.8 ms, $p = 0.033$) or odor-taste mixtures (349.2 ± 49.5 ms, $p = 0.012$). Next, we analyzed the duration of activity that was significantly greater than baseline (a measure of total excitation) or significantly lower than baseline (a measure of total suppression). Overall, the excited activity lasted significantly longer (716.2 ± 34.7 ms) than the responses suppressed by chemosensory stimuli (477.2 ± 27.5 ms; two-sample Kolmogorov–Smirnov test, K-S stat = 0.21, $p < 0.001$). Unlike response latency, there were no differences among stimulus categories in the duration of either excited activity (odors: 737.1 ± 74.5 ms, tastes: 742.6 ± 60.3 ms, mixtures: 685.0 ± 51.7 ms; Kruskal–Wallis, $H(2) = 0.3723$, $p = 0.8301$) or suppressed activity (odors: 528.2 ± 59.2 ms, tastes: 488.6 ± 49.9 ms, mixtures: 441.6 ± 39.3 ms; Kruskal–Wallis, $H(2) = 1.4805$, $p = 0.4770$). In summary, neuron activity was suppressed by stimuli more quickly, especially in response to odors, but exhibited excitation for a significantly longer time than suppression was observed.

Population decoding of chemosensory signals by the mediodorsal thalamus

Although the activity of individual neurons can represent specific features of chemosensory stimuli, neuronal networks are responsible for integrating and processing that information to guide behavior. We hypothesized that the heterogeneity displayed by the population of chemoselective neurons enables the accurate representation of the various chemosensory stimuli over time. We performed a population decoding analysis (see Materials and Methods for details) to examine whether the firing patterns of the ensemble of chemoselective neurons in the mediodorsal thalamus accurately encodes stimulus identity over time (Jezzini et al., 2013; Meyers, 2013; Liu and Fontanini, 2015; Bouaichi and Vincis, 2020). We began by analyzing how well the population activity of chemoselective neurons ($n = 85$) and nonchemoselective neurons ($n = 50$) represented the 12 intraoral stimuli during the 5 s after stimulus delivery. Figure 4*A* shows the average decoding performance of the two populations over time. The classification accuracy of the chemoselective population exceeded the chance level (8.3%) and significantly differed from that of the nonchemoselective population beginning 250 ms after stimulus delivery (permutation test, $p < 0.05$) and continuing for the entire 5-s window. As expected, the decoding performance of the nonchemoselective neurons showed that its population activity does not represent information about intraoral stimuli. These results are consistent with the population of chemoselective neurons encoding the identity of chemosensory signals originating from the mouth.

The confusion matrices in Figure 4*B* show the two population's average classification performances for each stimulus over the 5 s after intraoral delivery. White squares represent a classification accuracy less than chance (8.3%), and darker hues indicate better performance. The diagonal squares represent the proportion of trials for which the classifier correctly assigned the predicted stimulus (rows) to its true stimulus (columns). Off-diagonal squares indicate the proportion of trials where the predicted stimulus did not match the true stimulus (i.e., false predictions). The confusion matrix of the chemoselective population (Fig. 4*B*, left) shows that the classification accuracy for each stimulus is greatest along the diagonal (i.e., predicted stimulus matches the true stimulus) and reveals the predicted stimuli the classifier most often confused for each true stimulus. For example, the classifier most often correctly predicted citric acid but sometimes incorrectly predicted odor-taste mixtures containing citric acid. The proportion of trials where the predicted stimulus did not match the true stimulus (i.e., rows excluding the diagonal) was significantly greater for the nonchemoselective population (8.36 ± 0.17%) than that for the chemoselective population (6.09 ± 0.51%, Wilcoxon rank-sum, $Z = 6.78$, $p < 0.001$), indicating that the population activity of nonchemoselective neurons resulted in significantly more incorrect predictions than that for the chemoselective population.

Visual inspection of the confusion matrix for the chemoselective population (Fig. 4*B*) suggested that the classifier was more likely to "confuse" water, the odors, and the palatable stimuli (i.e., NaCl, sucrose, or an odor-taste mixture containing sucrose)

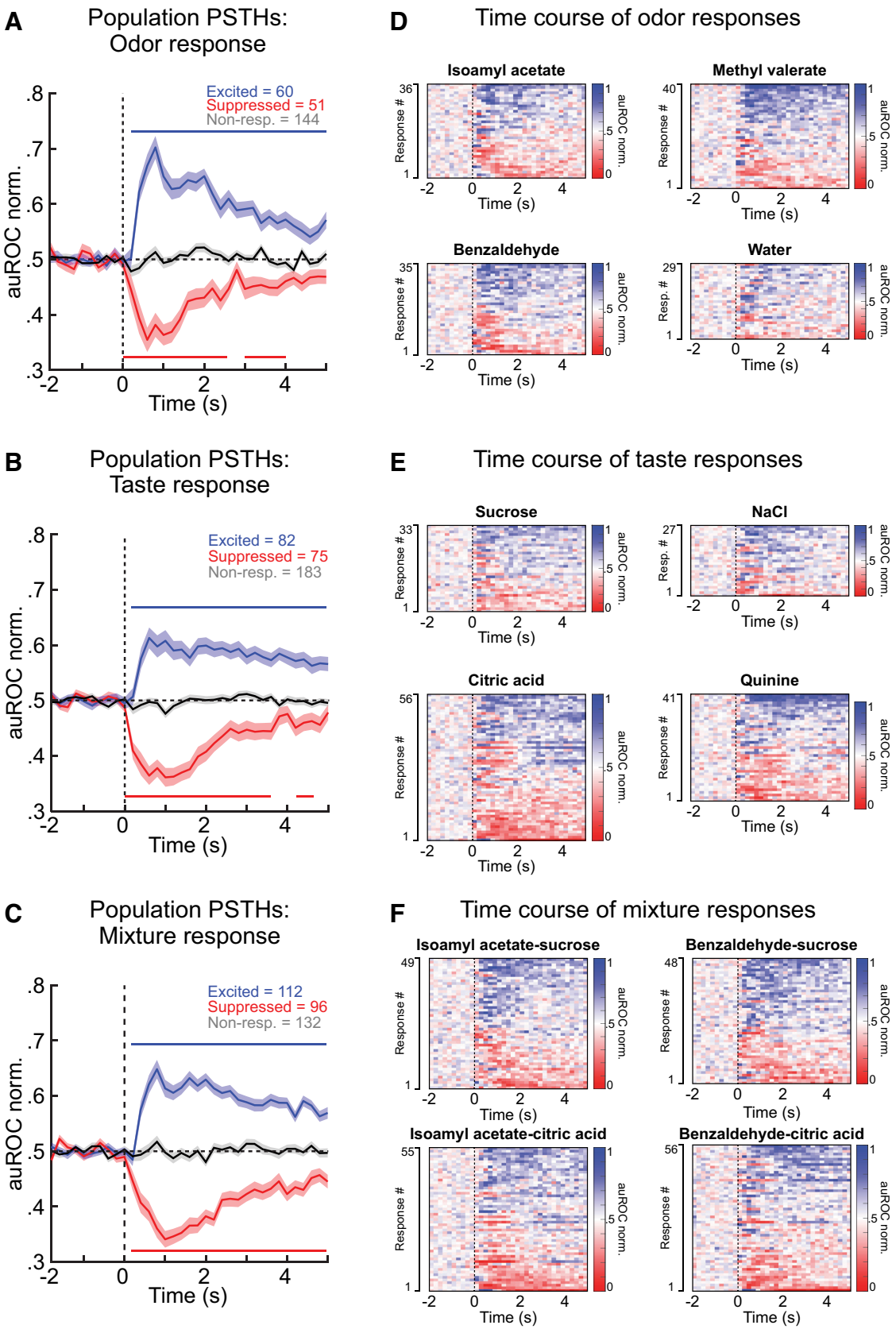

Figure 3. Intraoral chemosensory stimuli evoke excited and suppressed responses. ***A–C***, auROC-normalized (auROC-norm.) population PSTHs of the responses that showed excited (blue) or suppressed (red) activity or were nonresponsive (Non-resp., black) after the presentation of (***A***) odors, (***B***) tastes, and (***C***) odor-taste mixtures. Vertical dashed lines indicate stimulus delivery (time = 0). Horizontal dashed lines indicate baseline. The shaded area represents the SEM. Horizontal lines above (blue) and below (red) traces indicate when responses significantly differed from nonresponses (Wilcoxon rank-sum, $p < 0.05$). ***D–F***, Pseudocolored heat maps of each significant response to (***D***) odors, (***E***) tastes, and (***F***) odor-taste mixtures plotted in order from the most suppressed (red) to the most excited (blue) response for each stimulus.

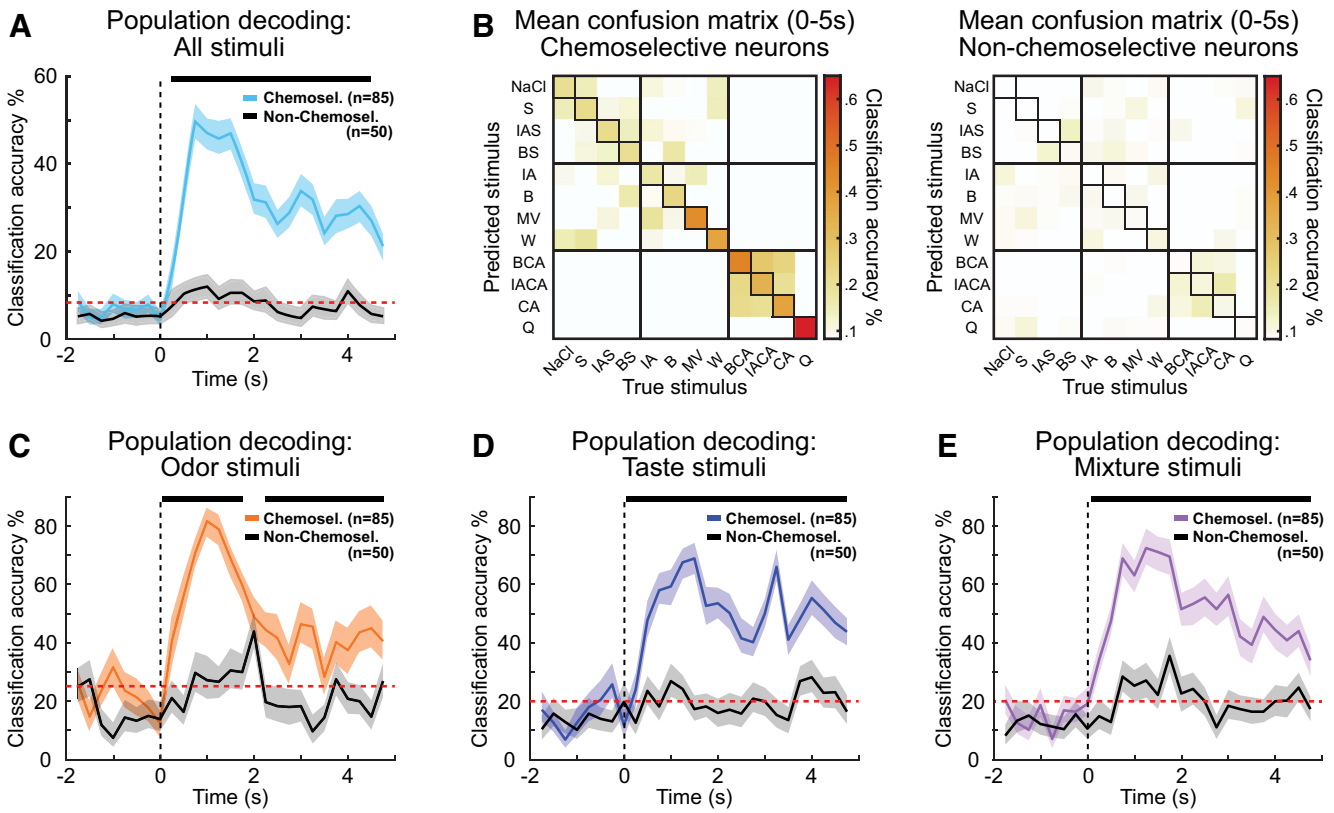

Figure 4. Population decoding of chemosensory signals by neurons in the mediodorsal thalamus. ***A***, The population decoding performance over time by the chemoselective neurons (Chemosel., $n = 85$) and nonchemoselective neurons (Non-Chemosel., $n = 50$) for all 12 intraoral stimuli. The red dashed line indicates chance level. The vertical dashed line indicates stimulus delivery (time = 0). The shaded area represents a 99.5% bootstrapped confidence interval. The horizontal black bar above the trace denotes bins when the classification accuracy significantly differed between the two populations (permutation test, $p < 0.05$). ***B***, Confusion matrices of the chemoselective (left) and nonchemoselective (right) populations showing the average classification accuracy over the 5 s after stimulus delivery. Colors represent the classification accuracy, with white squares representing performance less than chance (8.3%) and darker hues indicating a greater fraction of correct trials. The diagonal squares highlight the proportion of trials in which the classifier correctly assigned the predicted stimulus to the true stimulus. ***C–E***, The population decoding performance over time by the chemoselective and nonchemoselective populations for the three categories of chemosensory stimuli: (***C***) odors, (***D***) tastes, and (***E***) odor-taste mixtures.

with each other than with the unpalatable stimuli (i.e., citric acid, quinine, or an odor-taste mixture containing citric acid). This would suggest that the chemoselective population may represent palatability-related features of chemosensory stimuli. To determine whether false predictions were more likely to occur between similar groups of stimuli, we compared the proportion of trials where the predicted stimulus did not match the true stimulus (i.e., the off-diagonal squares) between the palatable stimuli, waters and odors, and unpalatable stimuli. When the classifier erroneously predicted a palatable stimulus (top four rows), the true stimulus was more likely to be another palatable stimulus (10.1 ± 1.4%, $p < 0.001$) or an odor or water (8.3 ± 1.1%, $p < 0.001$) than an unpalatable stimulus (1.8 ± 0.3%; Kruskal–Wallis, $H(2) = 27.52$, $p < 0.001$). When the classifier erroneously predicted an odor or water (middle four rows), the true stimulus was more likely to be another odor or water (8.1 ± 1.4%, $p = 0.002$) or a palatable stimulus (8.9 ± 1.2%, $p < 0.001$) than an unpalatable stimulus (1.5 ± 0.2%; Kruskal–Wallis, $H(2) = 28.50$, $p < 0.001$). However, when the classifier erroneously predicted an unpalatable stimulus (bottom four rows), the true stimulus was more likely to be another unpalatable stimulus (13.6 ± 2.9%; Kruskal–Wallis, $H(2) = 12.48$, $p < 0.001$) than either a palatable stimulus (3.1 ± 0.4%, $p = 0.022$) or an odor or water (2.8 ± 0.5%, $p = 0.002$). These results are consistent with the chemoselective population representing the palatability-related features of chemosensory stimuli.

Although the population activity of the chemoselective neurons accurately encoded the 12 intraoral stimuli, response similarities within the different chemosensory categories (e.g., tastes: NaCl and sucrose; odors: isoamyl acetate and methyl valerate; mixtures: benzaldehyde-citric acid and isoamyl acetate-citric acid) sometimes resulted in false predictions. Therefore, we next examined how well the population activity of chemoselective and nonchemoselective neurons decoded stimuli within each of the chemosensory categories. The odor decoding performance of the chemoselective population (Fig. 4*C*) showed an early onset, with a classification accuracy above chance level and significantly differing from that of the nonchemoselective population from the first bin after intraoral delivery (0–250 ms; permutation test, $p < 0.05$). The significant difference in classification accuracy between the two populations was briefly disrupted ~2 s after stimulus delivery before returning to significance for the remaining temporal window. The taste decoding performance of the chemoselective population (Fig. 4*D*) did not perform above the chance level until the second bin after intraoral delivery (250–500 ms) but significantly differed from that of the nonchemoselective population beginning from the first bin (0–250 ms; permutation test, $p < 0.05$). The classification accuracy remained above chance level and significantly different from that of the nonchemoselective population for the remaining temporal window. Similar to the decoding performance of odors, the odor-taste mixture decoding performance of the chemoselective population (Fig. 4*E*) showed an early onset, with a classification

accuracy above chance level and significantly differing from that of the nonchemoselective population from the first bin (0–250 ms; permutation test, $p < 0.05$). Similar to the decoding performance of tastes, the classification accuracy for odor-taste mixtures remained above chance level and was significantly different from that of the nonchemoselective population for the entire 5-s time frame. This population decoding analysis showed that the activity of chemoselective neurons differently represents the four odor-taste mixtures, despite them being composed of only two tastes (sucrose and citric acid) and two odors (isoamyl acetate and benzaldehyde).

Together, these data indicate that the ensemble of chemoselective neurons in the mediodorsal thalamus reliably encodes unimodal and multimodal chemosensory signals over time. Furthermore, the population activity evoked by water, odors, and palatable stimuli is more similar than that of the responses to unpalatable stimuli, suggesting that subpopulations of chemoselective neurons may preferentially represent information about stimulus identity or stimulus palatability.

Most chemoselective neurons respond to mixtures differently from one of their components

The odor-taste mixture decoding performance of the chemoselective population activity (Fig. 4*E*) suggested odor-taste mixtures are represented differently from their components. However, the activity evoked by the intraoral delivery of odor-taste mixtures may be similar to the odor and taste component alone. Visual inspection of raster plots and PSTHs suggested that a subset of chemoselective neurons responded differently to odor-taste mixtures compared with their individual odor or taste components (Fig. 5*A*). To determine which chemoselective neurons in the mediodorsal thalamus responded to odor-taste mixtures differently from their unimodal components, we performed an MCD analysis (see Materials and Methods for details). This analysis quantified the difference in firing rate across time between the neuronal response to an odor-taste mixture and the response to its odor component alone or its taste component alone. A response was considered significantly different when the evoked MCD score exceeded the mean of the eight baseline MCD scores ± six times the SD. Figure 5*B* shows the representative neuron's MCD score for the difference between the activity evoked by the mixture of isoamyl acetate-sucrose and isoamyl acetate alone (left) and the MCD score for the difference between the activity evoked by the mixture of benzaldehyde-sucrose and sucrose alone (right).

The MCD analysis revealed that nearly one-third of the odor-taste mixture responses (32.8%, 168/680) differed from at least one of their components (mixture-taste: isoamyl acetate-sucrose and sucrose: 19/85, 22.4%; benzaldehyde-sucrose and sucrose: 27/85, 31.8%; benzaldehyde-citric acid and citric acid: 16/85, 18.8%; isoamyl acetate-citric acid and citric acid: 14/85, 16.5%. mixture-odor: isoamyl acetate-sucrose and isoamyl acetate: 18/85, 21.2%; isoamyl acetate-citric acid and isoamyl acetate: 24/85, 28.2%; benzaldehyde-sucrose and benzaldehyde: 23/85, 27.1%; benzaldehyde-citric acid and benzaldehyde: 27/85, 31.8%). There was no difference between the proportion of mixture-taste MCD responses (76/168, 45.2%) and mixture-odor MCD responses (92/168, 54.8%; Fisher's exact test, $p = 0.102$). Because each MCD score represents the difference in firing rate between an odor-taste mixture and one of its components, a positive MCD score indicates that the mixture-evoked activity was higher than the component-evoked activity (Fig. 5*B*, right), while a negative MCD score indicates that the component-evoked activity was higher than the mixture-evoked activity (Fig. 5*B*, left). Next, we asked whether the significant response of each MCD score was because of higher mixture-evoked activity or higher component-evoked activity. We found that, overall, there were significantly more MCD responses with higher mixture-evoked activity (100/168; 59.5%) than higher component-evoked activity (68/168, 40.5%; Fisher's exact test, $p < 0.001$). There was a significant difference in the proportion of mixture-taste MCD responses with higher mixture-evoked activity (56/76, 73.7%) compared with those mixture-taste MCD responses with higher taste-evoked activity (20/76, 26.3%; Fisher's exact test, $p < 0.001$). However, there was no difference in the proportion of mixture-odor MCD responses with higher mixture-evoked activity (44/92, 47.8%) compared with those mixture-odor MCD responses with higher odor-evoked activity (48/92, 52.2%; $p = 0.66$).

We next determined how many neurons represented the 168 significant MCD responses (a neuron could have a maximum of eight significant MCD responses; four odor-taste mixtures compared with their odor and taste component). We found that 53 of the 85 (62.4%) chemoselective neurons accounted for the significant MCD responses. Of the 53 neurons, 21 (39.6%, 21/53) had odor-taste mixture responses that differed from both odor and taste responses, 23 (43.4%, 23/53) differed from odor responses alone, and 9 (17.0%, 9/53) differed from taste responses alone. Interestingly, we found no difference in the number of MCD responses for neurons with odor-taste mixture responses that differed from both odor (2.23 ± 0.23) and taste responses (2.61 ± 0.26), differed from odor responses alone (1.96 ± 0.22), or differed from taste responses alone (2.33 ± 0.33, Kruskal–Wallis, $H(3) = 3.904$, $p = 0.272$). These results indicate that mixture-odor and mixture-taste MCD responses were distributed across this chemoselective population, with most neurons representing multiple mixture-component differences. A total of 18 (34.0%,18/53) neurons responded to at least one mixture differently than both of that same mixture's components (isoamyl acetate-sucrose, isoamyl-acetate, and sucrose: 38.9%, 7/18; benzaldehyde-sucrose, benzaldehyde, and sucrose: 72.2%,13/18; benzaldehyde-citric acid, benzaldehyde, and citric acid: 33.3%, 6/18; isoamyl acetate-citric acid, isoamyl-acetate, and citric acid: 33.3%, 6/18).

To examine the time course of MCD responses, we calculated the average absolute difference in MCD (−2–5 s; 200-ms bins) for the significant MCD responses and the non-MCD responses (Fig. 5*C*). The average absolute MCD score was used to account for differences between odor-taste mixtures and their components regardless of whether the mixture or the component had the greater firing rate (Fig. 5*B*). This analysis revealed that significant MCD responses differed from baseline at 600 ms, peaked at 800 ms, and remained significantly above baseline for 3 s after stimulus delivery (Wilcoxon rank-sum, two consecutive significant bins, $p < 0.05$). The average absolute value of the non-MCD responses did not differ from baseline ($p > 0.05$). This analysis suggested that the difference between mixtures and their unimodal component is largely represented from ~0.5 to 3 s after stimulus delivery.

We used population decoding analysis to examine how well the activity of the neuron ensemble with odor-taste mixture responses that differed from at least one of its components (i.e., significant MCD) encoded the 12 intraoral stimuli over time. Figure 5*D* shows the average decoding performance over time of the population of chemoselective neurons with significant MCD responses ($n = 53$) and the non-MCD population ($n = 32$). The classification accuracy of the population with significant MCD

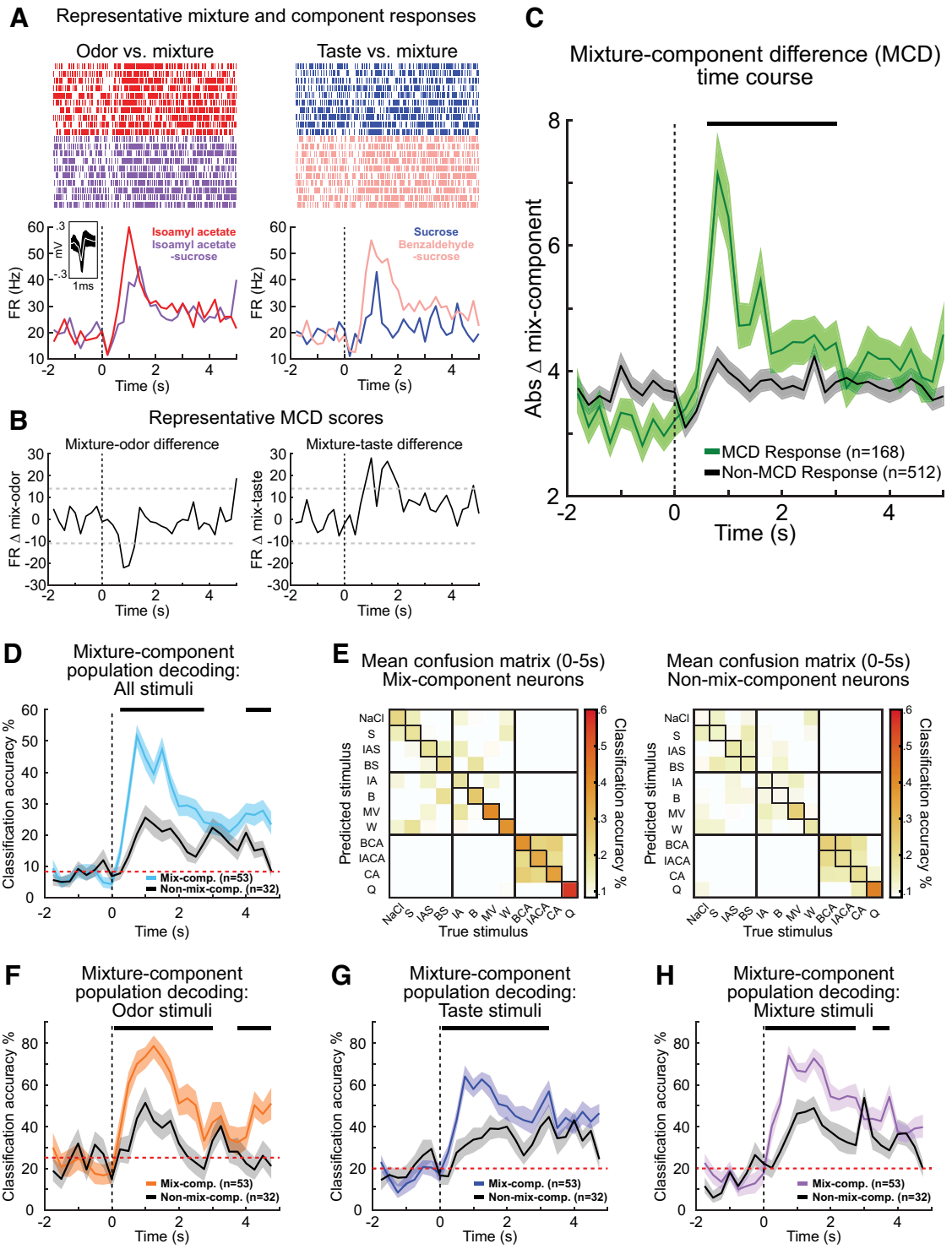

Figure 5. Most chemoselective neurons respond to mixtures differently than their odor or taste component. ***A***, Raster plots and PSTHs from a representative neuron in the mediodorsal thalamus illustrating the differences in activity evoked by mixtures and their components: isoamyl acetate-sucrose mixture versus isoamyl acetate alone (left) and benzaldehyde-sucrose mixture and sucrose alone (right). Vertical dashed lines indicate stimulus delivery (time = 0). Inset, The average action potential waveform. The extended data table (Extended Data Table 5-1) lists each of the 85 chemoselective neurons mean firing rate between 0.25–1 s for all 12 stimuli. ***B***, The MCD scores for the responses by the representative neuron. Left, The MCD score is the difference between the activity evoked by the mixture of isoamyl acetate-sucrose and the isoamyl acetate alone. Right, The MCD score is the difference between the activity evoked by the mixture of benzaldehyde-sucrose and sucrose alone (right). Vertical dashed lines indicate stimulus delivery (time = 0). Gray dashed lines indicate the significance threshold (baseline MCD score ± 6 times the SD). ***C***, Time course of the average absolute mixture-component difference (MCD) score for the 168 significant MCD responses (green line) and the 512 non-MCD responses (black line) from 2 s before to 5 s after intraoral delivery (200-ms bins). The significant MCD responses differ from baseline from 0.6 to 3 s (black bar) after stimulus delivery, and the non-MCD responses never differ from baseline. The shaded area represents the SEM. ***D***, The population decoding performance for all 12 intraoral stimuli over time by the ensembles of chemoselective neurons with MCD responses (Mix-comp., $n = 53$) and non-MCD responses (Non-mix-comp., $n = 32$). The red dashed line indicates chance level. The vertical dashed line indicates stimulus delivery (time = 0). The shaded area represents a 99.5% bootstrapped confidence interval. The horizontal black bar above the trace denotes bins when the classification accuracy significantly differed between the two populations (permutation test, $p < 0.05$). ***E***, Confusion matrices of the MCD neurons (left) and non-MCD neurons (right) showing the average classification accuracy over the 5 s after stimulus delivery. Color is used to represent the classification accuracy, with white squares representing performance less than chance and darker hues indicating a greater fraction of correct trials. The diagonal squares highlight the proportion of trials in which the

responses exceeded the chance level beginning in the first bin (0–250 ms), while the non-MCD population did not exceed the chance level until the second bin after intraoral delivery (250–500 ms). Both populations performed better than chance for the remainder of the temporal window, but the classification accuracy of the MCD population was significantly better than that of the non-MCD population for ~3 s after stimulus delivery (permutation test, $p < 0.05$). The confusion matrices in Figure 5*E* show the average classification performance for each stimulus during the 5 s after stimulus delivery of the population with significant MCD responses (left) and the non-MCD population (right). The proportion of trials where the predicted stimulus did not match the true stimulus (i.e., the rows excluding the diagonal) was significantly greater for the non-MCD population (7.43 ± 0.35) than that for the population with significant MCD responses (6.32 ± 0.46, Wilcoxon rank-sum, $Z = 3.79$, $p < 0.001$), indicating that the population activity of the non-MCD neurons resulted in significantly more incorrect predictions than that for neurons with significant MCD responses.

Next, we sought to determine whether the decoding performance of the two populations differed within each chemosensory category. Figure 5*F–H* shows the decoding performance of the population of chemoselective neurons with significant MCD responses and the non-MCD population for the three categories of chemosensory stimuli. Decoding performance by the population with significant MCD responses showed an early onset for all three chemosensory categories with classification accuracies above chance level and significantly differing from that of the non-MCD population beginning in the first bin (0–250 ms; permutation test, $p < 0.05$). The classification accuracy of the non-MCD population did not exceed the chance level until the second bin (250–500 ms) for tastes (Fig. 5*G*) and odor-taste mixtures (Fig. 5*H*) or until the third bin (500–750 ms) for odors (Fig. 5*F*). For all three stimulus categories, the significant differences in decoding performance between the MCD and non-MCD populations were maintained for ~3 s after stimulus delivery.

Taken together, these results show that most chemoselective neurons in the mediodorsal thalamus respond to odor-taste mixtures differently than their odor or taste component, with chemosensory information largely represented during the first 3 s after stimulus delivery.

A subset of chemoselective neurons represents the palatability-related features of tastes

Tastes have intrinsic value, and rodents consume palatable tastes and avoid unpalatable ones. It is well established that brain regions important for chemosensory processing and feeding-related behaviors represent the chemical and palatability-related features of tastes (Fontanini et al., 2009; Piette et al., 2012; Sadacca et al., 2012; Jezzini et al., 2013; Li et al., 2013; Liu and Fontanini, 2015; Samuelsen and Fontanini, 2017). The decoding performance and confusion matrix of the chemoselective population activity (Fig. 4*A*,*B*) suggested that a subset of neurons may encode the palatability-related features of chemosensory stimuli. Therefore, we calculated a palatability index (PI; see Materials and Methods for details) to determine whether neurons in the mediodorsal thalamus represent the palatability-related features of tastes, meaning that tastes belonging to similar hedonic categories evoke similar responses (e.g., sucrose/NaCl vs citric acid/quinine). This analysis quantified the differences in activity between tastes of similar palatability (sucrose/NaCl, citric acid/quinine) and tastes of opposite palatability (sucrose/quinine, sucrose/citric acid, NaCl/quinine, NaCl/citric acid). A chemoselective neuron was considered to represent taste palatability when it had a positive PI score (i.e., it responded similarly to tastes with similar hedonic value but differently to tastes with opposite hedonic value) and the evoked PI score exceeded the mean ± six times the SD of the baseline (Bouaichi and Vincis, 2020).

This analysis revealed that the activity of more than a quarter (27.1%, 23/85) of the chemoselective neurons represented palatability-related features of tastes [Fig. 6*A*, representative examples auROC normalized firing rate (top) and PI scores (bottom)]. To examine the temporal evolution of palatability-related activity, we calculated the average PI score (−2–5 s; 200-ms bins) for the populations of palatability-related ($n = 23$) and nonpalatability-related neurons ($n = 62$). Figure 6*B* shows that the mean PI score of the palatability-related neurons began to significantly differ from baseline after 1.2 s and peaked 2 s after stimulus delivery (Wilcoxon rank-sum, two consecutive significant bins, $p < 0.05$). The mean PI score of the nonpalatability-related population did not differ from baseline ($p > 0.05$).

Because, by definition, neurons in the palatability-related population must respond similarly to tastes with similar palatability, the nonpalatability-related population of chemoselective neurons should better represent the identity of chemosensory stimuli over time. Figure 6*C* shows the average decoding performance for all 12 stimuli over time for the palatability-related ($n = 23$) and nonpalatability-related ($n = 62$) populations of chemoselective neurons. The classification accuracy of the nonpalatability-related population exceeded the chance level beginning in the first bin (0–250 ms), but the classification accuracy of the palatability-related population did not exceed the chance level until the second bin after intraoral delivery (250–500 ms). Both populations performed better than chance level for the remainder of the 5-s window. However, the classification accuracy of the nonpalatability-related population was significantly better than that of the palatability-related population between 0.25 and 1 s after stimulus delivery (permutation test, $p < 0.05$). The confusion matrices in Figure 6*D* show the average classification performance for each stimulus during the 5 s after intraoral delivery in the palatability-related (left) and nonpalatability-related (right) populations of chemoselective neurons. There was no difference between the two populations in the proportion of trials in which the predicted stimulus did not match the true stimulus (i.e., the rows excluding the diagonal; $6.99 \pm 0.48\%$ vs $6.74 \pm 0.41\%$, Wilcoxon rank-sum, $Z = 0.27$, $p = 0.79$), indicating that the two populations performed similarly overall despite the differences in the classification accuracy between 0.25 and 1 s after stimulus delivery.

As predicted, the decoding performance of the nonpalatability-related population activity was significantly better than that of the palatability-related population activity. Therefore, we expected that a comparison of the decoding performance of the two populations for each chemosensory category would reveal worse classification accuracy of the palatability-related population for tastes but better accuracy for odors and odor-taste

←

classifier correctly assigned the predicted stimulus to its true stimulus. ***F–H***, The population decoding performance over time by MCD neurons and non-MCD neurons for the three categories of chemosensory stimuli: (***F***) odors, (***G***) tastes, and (***H***) odor-taste mixtures. Note that both populations had decoding performances above chance level (red dashed line) but with different temporal profiles.

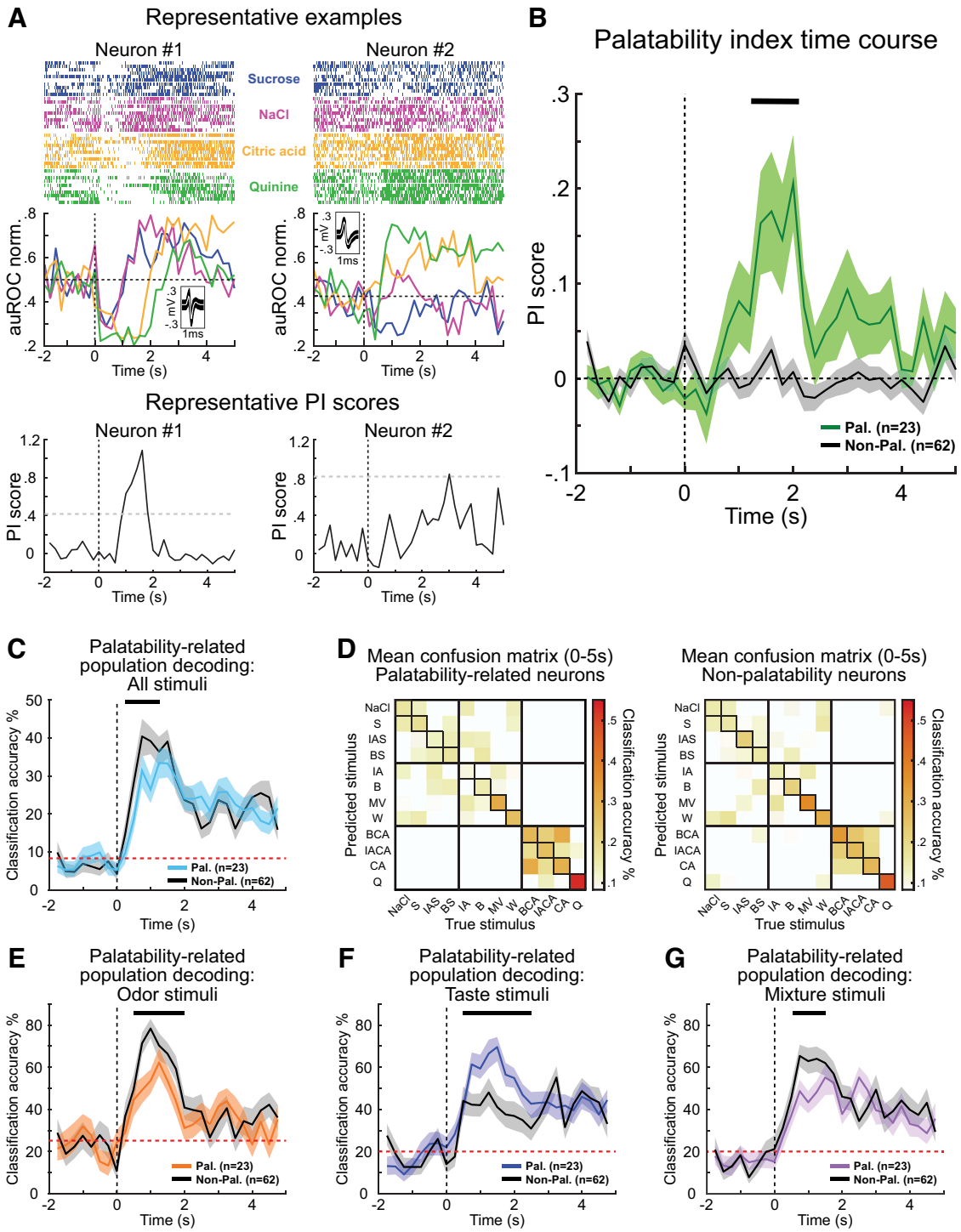

Figure 6. Processing of taste palatability by neurons in the mediodorsal thalamus. ***A***, Top, Raster plots and auROC normalized PSTHs from two neurons in the mediodorsal thalamus that represent the palatability-related features of tastes. Vertical dashed lines indicate stimulus delivery (time = 0). Horizontal dashed lines indicate baseline. Insets, Average action potential waveforms for each neuron. Bottom, Palatability Index (PI) scores of the two representative neurons. Gray dashed lines indicate the significance threshold (baseline PI score ± 6 times the SD). The extended data table (Extended Data Table 6-1) lists each of the 85 chemoselective neurons mean firing rate between 2 and 2.5 s for all 12 stimuli. ***B***, Time course of the average palatability index (PI) score of the 23 palatability-related neurons (Pal., green line) and 62 nonpalatability neurons (Non-Pal., black line) 2 s before to 5 s after intraoral delivery (200-ms bins). The response of the palatability-related population significantly differs from baseline from 1.4 to 2 s (black bar) after stimulus delivery, while the average PI score of the nonpalatability population never differs from baseline. The vertical dashed line indicates stimulus delivery (time = 0). The horizontal dashed line indicates baseline. The shaded area represents the SEM. ***C***, The population decoding performance for all 12 intraoral stimuli over time by palatability-related ($n = 23$) and nonpalatability-related neurons ($n = 62$). Note that the decoding performance for the 12 stimuli by the population of nonpalatability-related neurons is significantly greater than that of the palatability-related population (black bar; permutation test, $p < 0.05$). The red dashed line indicates chance level. The vertical dashed line indicates stimulus delivery (time = 0). The shaded area represents a 99.5% bootstrapped confidence interval. ***D***, Confusion matrices of the palatability-related (left) and nonpalatability-related neurons (right) showing the average classification accuracy over the 5 s after stimulus delivery. Colors represent the classification accuracy, with white squares representing performance less than chance and darker hues indicating a greater fraction of correct trials. The diagonal squares highlight the proportion in which the classifier correctly assigned the predicted stimulus to its true stimulus. ***E–G***, The population decoding performance over time by the palatability-related and nonpalatability-related neurons for the three categories of chemosensory stimuli: (***E***) odors, (***F***) tastes, and (***G***) odor-taste mixtures.

mixtures. Figure 6*E–G* shows the decoding performance for the three categories of chemosensory stimuli in the palatability-related and nonpalatability-related populations. Counter to our prediction, the decoding performance of palatability-related population activity was significantly better than that of the nonpalatability-related neuron activity for tastes (Fig. 6*F*) but worse for odors (Fig. 6*E*) and odor-taste mixtures (Fig. 6*G*).

Interestingly, these population decoding analyses revealed that the poorer decoding performance for all 12 stimuli by the palatability-related population (Fig. 6*C*) was not because of confusion between taste stimuli. In fact, the taste decoding performance of the palatability-related population was significantly better than that of the nonpalatability population (Fig. 6*F*). An alternative reason for the poorer decoding performance by the palatability-related population could be because of similar population activity evoked by individual odor and taste stimuli previously experienced together as an odor-taste mixture. Behavioral studies have shown that multiple days of experience with odor-taste mixtures establishes odor-taste associations that inform consummatory choice (Sakai and Yamamoto, 2001; McQueen et al., 2020). For example, rats that are exposed to mixtures of isoamyl acetate-sucrose and benzaldehyde-citric acid prefer to consume water containing isoamyl acetate rather than water containing benzaldehyde. However, rats that are exposed to mixtures with the opposite pairs, such as isoamyl acetate-citric acid and benzaldehyde-sucrose, prefer to consume water containing benzaldehyde rather than water containing isoamyl acetate (McQueen et al., 2020). These powerful associations are resistant to extinction (Sakai and Imada, 2003; Albertella and Boakes, 2006; Yeomans et al., 2006; González et al., 2016) and link the odor with the taste quality and value (Fanselow and Birk, 1982; Holder, 1991; Stevenson et al., 1995; Prescott et al., 2004; Gautam and Verhagen, 2010; Green et al., 2012; McQueen et al., 2020). To avoid variability across sessions related to learning of odor-taste associations, we provided rats with experience to isoamyl acetate-sucrose and benzaldehyde-citric acid mixtures. Because of this odor-taste mixture experience, it is possible that the poorer decoding performance by the palatability-related neurons was because of similarities in the population activity between isoamyl acetate and sucrose and those between benzaldehyde and citric acid.

To investigate the relationship between previously presented odor-taste pairs, we trained the classifier with the population activity evoked by sucrose and citric acid (true stimulus) and elicited predictions based on the population activity evoked by isoamyl acetate or benzaldehyde (predicted stimulus). The classification accuracy of the taste-trained classifier should exceed chance level if the activity evoked by a taste is similar to the activity evoked by its previously paired-odor. Figure 7*A* shows the taste-trained decoding performance of the palatability-related and nonpalatability-related neurons. The classification accuracy of the palatability-related population performed better than chance and was significantly better than that of the nonpalatability-related population during two time frames, 0.25–1 and 2–2.5 s after stimulus delivery (permutation test, $p < 0.05$). Next, we tested the opposite relationship by training the classifier with the population activity evoked by isoamyl acetate and benzaldehyde (true stimulus) and elicited predictions based on the population activity evoked by sucrose and citric acid (predicted stimulus; Fig. 7*C*). As with the taste-trained classifier above, the odor-trained classifier revealed that the classification accuracy of the palatability-related population performed better than chance and was significantly better than that of the nonpalatability-related population during the time frames of 0.25–1 and 1.75–2.5 s after stimulus delivery (permutation test, $p < 0.05$). The average classification accuracies of the two populations during the peak decoding performance (0.25–1 s) are represented by the confusion matrices in Figure 7*B* and *D*. Together, the results of the taste-trained classifier and odor-trained classifier showed that the proportion of trials during the initial peak (0.25–1 s after stimulus delivery), where the predicted stimulus did not match the true stimulus (i.e., false predictions), were significantly greater for the nonpalatability-related population (55.4 ± 4.3%) than those for the palatability-related population (27.0 ± 3.6%, Wilcoxon rank-sum, $Z = 3.47$, $p < 0.001$). Thus, the population activity of the nonpalatability-related neurons resulted in significantly more incorrect predictions than that of the palatability-related population. These results suggest that the poorer overall decoding performance by the palatability-related neurons during the 0.25–1 s after stimulus delivery (Fig. 6*C*) is related to the similar responses evoked by the components of previously experienced odor-taste mixtures.

In summary, the chemoselective population of neurons in the mediodorsal thalamus is broadly responsive to intraoral chemosensory stimuli and responds to odor-taste mixtures differently than an odor or taste alone. This chemoselective population contains a subset of neurons that represents the palatability-related features of tastes that may also represent associations between experienced odor-taste pairs. Overall, the above findings demonstrate that chemoselective neurons in the mediodorsal thalamus dynamically encode chemosensory signals originating from the mouth.

Discussion

The thalamic subnuclei can be divided into two categories based on their functional connections with subcortical and cortical areas. First-order thalamic nuclei primarily process peripheral sensory input from subcortical regions before relaying it to the cortex, while higher-order thalamic nuclei process and communicate information between cortical areas (Sherman, 2016; Nakajima and Halassa, 2017; Halassa and Sherman, 2019). Higher-order thalamic areas, such as the mediodorsal thalamus, are thought to modulate, synchronize, and transmit behaviorally-relevant information between sensory and prefrontal cortical areas (Theyel et al., 2010; Saalmann et al., 2012; Stroh et al., 2013; Mease et al., 2016; Zhou et al., 2016; Schmitt et al., 2017; Rikhye et al., 2018). By sustaining communication across cortical regions, these cortico-thalamo-cortical (i.e., transthalamic) circuits separate potentially overlapping information and enable rapid behavioral changes based on environmental demands (Saalmann, 2014; Sherman, 2016; Rikhye et al., 2018). Given its connectivity, the mediodorsal thalamus may perform a similar function by communicating behaviorally-relevant chemosensory information between prefrontal cortical areas and principal regions of the olfactory and gustatory systems (Price and Slotnick, 1983; Kuroda et al., 1992; Ray and Price, 1992; Shi and Cassell, 1998; Kuramoto et al., 2017; Pelzer et al., 2017). However, a crucial step to understanding its role in chemosensory processing is determining how neurons represent orally-sourced odor, taste, and odor-taste mixture signals. Using tetrode recordings in behaving rats, our results indicate that most mediodorsal thalamus neurons respond broadly across intraoral stimuli with time-varying multiphasic changes in activity. Furthermore, we demonstrate that the population activity of

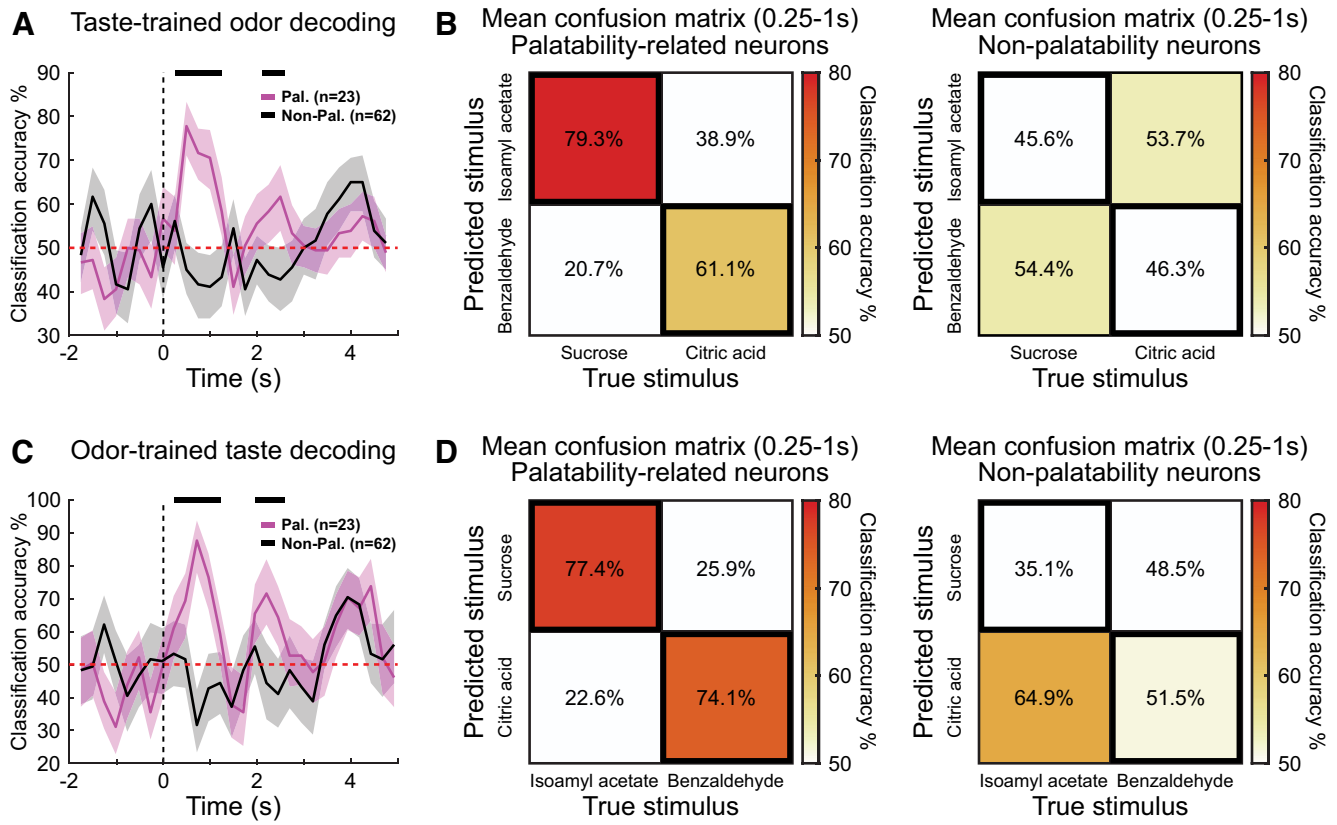

Figure 7. The population activity of palatability-related neurons represents the association between previously experienced odor-taste pairs. ***A***, Population decoding performance over time of the palatability-related (Pal., $n = 23$) and nonpalatability-related neurons (Non-Pal., $n = 62$) when responses to sucrose and citric acid were used to train the classifier (true stimulus), but testing it with responses to isoamyl acetate and benzaldehyde (predicted stimulus). The vertical dashed line indicates stimulus delivery (time = 0). The red dashed line indicates chance level performance (50%). The shaded area represents a 99.5% bootstrapped confidence interval. The horizontal black bar above the trace denotes bins in which the classification accuracy significantly differed between the two populations (permutation test, $p < 0.05$). ***B***, Confusion matrices showing the average classification accuracy during the initial peak 0.25–1 s after stimulus delivery for the palatability-related neurons (left) and nonpalatability-related neurons (right). Colors represent the classification accuracy, with darker hues indicating a greater fraction of correct trials. The diagonal highlights the proportion of trials in which the classifier correctly assigned the paired odor stimulus (predicted stimulus) to the correct paired taste (true stimulus). ***C***, Population decoding performance when responses to isoamyl acetate and benzaldehyde were used to train the classifier (true stimulus), but testing it with responses to sucrose and citric acid (predicted stimulus). ***D***, Confusion matrices showing the average classification accuracy during the initial peak 0.25–1 s after stimulus delivery for the palatability-related neurons (left) and nonpalatability-related neurons (right). The diagonal highlights the proportion of trials in which the classifier correctly assigned the paired taste (predicted stimulus) to the correct paired odor (true stimulus).

chemoselective neurons reliably encodes unimodal and multimodal chemosensory signals over time, representing both stimulus identity and stimulus palatability. Altogether, our findings further demonstrate the multidimensionality of the mediodorsal thalamus and provide novel evidence of its involvement in processing chemosensory information important to ingestive behaviors.

As a multimodal region, the mediodorsal thalamus responds to visual, auditory, somatosensory, and olfactory stimuli, but its role in processing gustatory signals is unknown (Yarita et al., 1980; Imamura et al., 1984; Oyoshi et al., 1996; Yang et al., 2006; Courtiol and Wilson, 2016). To our knowledge, the only study to provide evidence of taste-evoked activity in the mediodorsal thalamus showed that neurons responded to sucrose given as a reward for the correct choice in a sensory-discrimination task (Oyoshi et al., 1996). In addition to using only one taste stimulus, the complex nature of the task prevented determining whether responses were somatosensory, reward, or taste dependent. The present results are the first to demonstrate how neurons in the mediodorsal thalamus process the sensory and palatability-related features of tastes. Half of the total population of recorded neurons responded to the intraoral delivery of taste stimuli, with the majority of this chemoselective population responding to multiple taste qualities (i.e., broadly tuned). This population also reflected possible differences between palatable and unpalatable tastes, with a significantly greater proportion of neurons responding to citric acid than to either sucrose or NaCl, but not to quinine.

Many electrophysiological studies of cortical and subcortical regions throughout the gustatory system, including the gustatory thalamus, lateral hypothalamus, basolateral amygdala, central amygdala, gustatory cortex, and prefrontal cortex, have demonstrated that neurons encode taste palatability (Katz et al., 2001; Fontanini et al., 2009; Sadacca et al., 2012; Jezzini et al., 2013; Li et al., 2013; Samuelsen and Fontanini, 2017). Thus, we expected that mediodorsal thalamus neurons would also represent the palatability-related features of tastes. Similar to previous studies, we used a PI analysis to identify neurons that represent taste palatability and examine the temporal evolution of palatability-related activity in the mediodorsal thalamus. More than one-quarter of chemoselective neurons represented taste palatability, with palatability-related information primarily represented 1.2–2 s after stimulus delivery. Population decoding analyses of the 12 intraoral stimuli showed that the neurons representing the palatability-related features of tastes performed significantly worse than the remaining chemoselective population ~0.25–1 s after stimulus delivery. Surprisingly, this deficit in decoding performance was not because of poor taste coding but was likely caused by

"confusion" between the components of experienced odor-taste mixtures.

Because odor-taste mixture experience generates associations between the quality and value of an odor and a taste (Fanselow and Birk, 1982; Holder, 1991; Stevenson et al., 1995; Prescott et al., 2004; Gautam and Verhagen, 2010; Green et al., 2012; McQueen et al., 2020), we hypothesized that the deficit in overall decoding performance by the palatability-related population may be because of similar responses evoked by the components of experienced odor-taste mixtures. When training the classifier with the activity evoked by paired tastes but eliciting predictions using the activity evoked by paired odors (and vice versa), the peak decoding performance of odor-taste pairs occurred simultaneously with the deficit in the overall decoding performance, ~0.25–1 s after stimulus delivery. Although our results are consistent with the subpopulation of neurons that represents taste palatability also representing the relationship between experienced odor-taste pairs, it is possible that the response similarities observed represent an innate relationship between sucrose and isoamyl acetate and between citric acid and benzaldehyde. Future experiments employing a larger battery of odor-taste mixtures would help to elucidate whether mediodorsal thalamus neurons represent associations between experienced odor-taste pairs.

Convergence of chemosensory signals occurs in numerous subcortical and cortical areas (Di Lorenzo and Garcia, 1985; Maier et al., 2012; Escanilla et al., 2015; Maier, 2017; Samuelsen and Fontanini, 2017). These multimodal responses are thought to enhance detectability and discriminability across the network to better represent behaviorally-relevant environmental features (Ohshiro et al., 2011). The population activity of mediodorsal thalamus neurons accurately classified the four odor-taste mixtures, even when they consisted of only two odors and two tastes. Furthermore, the MCD analysis showed that nearly two-thirds of chemoselective neurons responded to an odor-taste mixture differently than at least one of its odor or taste components. This means that one-third of chemoselective neurons responded similarly to odor-taste mixtures and their components, suggesting that some chemoselective neurons faithfully represent individual odors and tastes even when they are presented as part of an odor-taste mixture. This coding scheme would allow ensembles of neurons in the mediodorsal thalamus to consistently represent unimodal information, while enabling flexibility when responding to multimodal signals. Alternatively, experience itself may be how neurons disambiguate mixtures with overlapping representations of odors and tastes. Future studies using novel odor-taste pairs for every session would allow determination of whether the convergent representation across mixtures is experience-dependent or a summation of olfactory and gustatory signals.

Although identifying the sources of chemosensory input to the mediodorsal thalamus is outside the scope of this study, the temporal dynamics of chemosensory-evoked activity indicate likely sources. The thalamic representation of chemosensory information is rapid and persistent, with responses to the various stimuli mostly overlapping in time. Chemoselective neurons begin to represent the chemical identity of odor-containing stimuli (odors and odor-taste mixtures) ~250 ms after intraoral delivery but take an additional ~250 ms to encode the identity of tastes alone. However, the palatability-related features of tastes are represented by a neuron subpopulation much later, between ~1.2 and 2 s after stimulus delivery. These response dynamics indicate the piriform cortex, gustatory cortex, and basolateral amygdala as likely sources of chemosensory input to the mediodorsal thalamus.

Both chemosensory cortical areas project to the mediodorsal thalamus and represent stimulus identity more quickly, where the piriform cortex encodes odor identity in ~100 ms (Bolding and Franks, 2017) and the gustatory cortex encodes taste identity in ~175–250 ms (Katz et al., 2001; Jezzini et al., 2013; Bouaichi and Vincis, 2020). However, another cortical region with dense reciprocal connections to the mediodorsal thalamus, the medial prefrontal cortex, does not represent taste identity until ~575 ms after intraoral delivery (Jezzini et al., 2013). Therefore, it is unlikely that the medial prefrontal cortex is a source of chemosensory input, but it may represent an important cortical feedback site for chemosensory information to the mediodorsal thalamus. Similar network interactions may be responsible for communicating the palatability-related features of tastes, as both the basolateral amygdala and gustatory cortex form dense reciprocal connections and represent the palatability-related features of tastes faster than the mediodorsal thalamus (Katz et al., 2001; Fontanini et al., 2009; Jezzini et al., 2013; Samuelsen and Fontanini, 2017). Together, the temporal dynamics of chemosensory processing suggest a mechanism whereby the mediodorsal thalamus receives chemosensory information from the piriform cortex, gustatory cortex, and/or basolateral amygdala, while dynamic multiphasic activity arises via recurrent interactions with prefrontal cortical areas. This transthalamic circuit could facilitate large-scale integration of chemosensory information across multiple cortical circuits (Saalmann, 2014). Future studies selectively targeting neuronal populations with cell-specific viral manipulations (e.g., optogenetics) would help to identify the contribution of these regions to chemosensory processing by the mediodorsal thalamus.

In summary, despite its robust connectivity with olfactory and gustatory areas, involvement in olfactory-dependent behaviors, and importance for the perception of flavors, the mediodorsal thalamus remains an understudied area of network processing of chemosensory information. Our results show that mediodorsal thalamus neurons dynamically encode the sensory and palatability-related features of chemosensory signals originating from the mouth. Future studies probing cortico-thalamo-cortical interactions in behaving animals are necessary to determine the contribution of the mediodorsal thalamus to chemosensory-dependent behaviors.

References

Aimé P, Duchamp-Viret P, Chaput MA, Savigner A, Mahfouz M, Julliard AK (2007) Fasting increases and satiation decreases olfactory detection for a neutral odor in rats. Behav Brain Res 179:258–264.

Albertella L, Boakes RA (2006) Persistence of conditioned flavor preferences is not due to inadvertent food reinforcement. J Exp Psychol Anim Behav Process 32:386–395.

Alcaraz F, Fresno V, Marchand AR, Kremer EJ, Coutureau E, Wolff M (2018) Thalamocortical and corticothalamic pathways differentially contribute to goal-directed behaviors in the rat. Elife 7:e32517.

Bamji-Stocke S, Biggs BT, Samuelsen CL (2018) Experience-dependent c-Fos expression in the primary chemosensory cortices of the rat. Brain Res 1701:189–195.

Bolding KA, Franks KM (2017) Complementary codes for odor identity and intensity in olfactory cortex. Elife 6:e22630.

Bolkan SS, Stujenske JM, Parnaudeau S, Spellman TJ, Rauffenbart C, Abbas AI, Harris AZ, Gordon JA, Kellendonk C (2017) Thalamic projections sustain prefrontal activity during working memory maintenance. Nat Neurosci 20:987–996.

Bouaichi CG, Vincis R (2020) Cortical processing of chemosensory and hedonic features of taste in active licking mice. J Neurophysiol 123:1995–2009.

Cohen JY, Haesler S, Vong L, Lowell BB, Uchida N (2012) Neuron-type-specific signals for reward and punishment in the ventral tegmental area. Nature 482:85–88.

Courtiol E, Wilson DA (2014) Thalamic olfaction: characterizing odor processing in the mediodorsal thalamus of the rat. J Neurophysiol 111:1274–1285.

Courtiol E, Wilson DA (2016) Neural representation of odor-guided behavior in the rat olfactory thalamus. J Neurosci 36:5946–5960.

Courtiol E, Neiman M, Fleming G, Teixeira CM, Wilson DA (2019) A specific olfactory cortico-thalamic pathway contributing to sampling performance during odor reversal learning. Brain Struct Funct 224:961–971.

Di Lorenzo PM, Garcia J (1985) Olfactory responses in the gustatory area of the parabrachial pons. Brain Res Bull 15:673–676.

Eichenbaum H, Shedlack KJ, Eckmann KW (1980) Thalamocortical mechanisms in odor-guided behavior: I. Effects of lesions of the mediodorsal thalamic nucleus and frontal cortex on olfactory discrimination in the rat. Brain Behav Evol 17:255–275.

Escanilla OD, Victor JD, Di Lorenzo PM (2015) Odor-taste convergence in the nucleus of the solitary tract of the awake freely licking rat. J Neurosci 35:6284–6297.

Fanselow MS, Birk J (1982) Flavor-flavor associations induce hedonic shifts in taste preference. Anim Learn Behav 10:223–228.

Fontanini A, Grossman SE, Figueroa JA, Katz DB (2009) Distinct subtypes of basolateral amygdala taste neurons reflect palatability and reward. J Neurosci 29:2486–2495.

Fredericksen KE, McQueen KA, Samuelsen CL (2019) Experience-dependent c-Fos expression in the mediodorsal thalamus varies with chemosensory modality. Chem Senses 44:41–49.

Gardner MPH, Fontanini A (2014) Encoding and tracking of outcome-specific expectancy in the gustatory cortex of alert rats. J Neurosci 34:13000–13017.

Gautam SH, Verhagen JV (2010) Evidence that the sweetness of odors depends on experience in rats. Chem Senses 35:767–776.

Gautam SH, Verhagen JV (2012) Direct behavioral evidence for retronasal olfaction in rats. PLoS One 7:e44781.

González F, Morillas E, Hall G (2016) The extinction procedure modifies a conditioned flavor preference in nonhungry rats only after revaluation of the unconditioned stimulus. J Exp Psychol Anim Learn Cogn 42:380–390.

Green BG, Nachtigal D, Hammond S, Lim J (2012) Enhancement of retronasal odors by taste. Chem Senses 37:77–86.

Halassa MM, Sherman SM (2019) Thalamocortical circuit motifs: a general framework. Neuron 103:762–770.

Holder MD (1991) Conditioned preferences for the taste and odor components of flavors: blocking but not overshadowing. Appetite 17:29–45.

Imamura K, Onoda N, Takagi SF (1984) Odor response characteristics of thalamic mediodorsal nucleus neurons in the rabbit. Jpn J Physiol 34:55–73.

Jezzini A, Mazzucato L, La Camera G, Fontanini A (2013) Processing of hedonic and chemosensory features of taste in medial prefrontal and insular networks. J Neurosci 33:18966–18978.

Jones LM, Fontanini A, Sadacca BF, Miller P, Katz DB (2007) Natural stimuli evoke dynamic sequences of states in sensory cortical ensembles. Proc Natl Acad Sci U S A 104:18772–18777.

Julliard AK, Chaput MA, Apelbaum A, Aimé P, Mahfouz M, Duchamp-Viret P (2007) Changes in rat olfactory detection performance induced by orexin and leptin mimicking fasting and satiation. Behav Brain Res 183:123–129.

Katz DB, Simon SA, Nicolelis MAL (2001) Dynamic and multimodal responses of gustatory cortical neurons in awake rats. J Neurosci 21:4478–4489.

Kawagoe T, Tamura R, Uwano T, Asahi T, Nishijo H, Eifuku S, Ono T (2007) Neural correlates of stimulus-reward association in the rat mediodorsal thalamus. Neuroreport 18:683–688.

Kuramoto E, Pan S, Furuta T, Tanaka YR, Iwai H, Yamanaka A, Ohno S, Kaneko T, Goto T, Hioki H (2017) Individual mediodorsal thalamic neurons project to multiple areas of the rat prefrontal cortex: a single neuron-tracing study using virus vectors. J Comp Neurol 525:166–185.

Kuroda M, Murakami K, Kishi K, Price JL (1992) Distribution of the piriform cortical terminals to cells in the central segment of the mediodorsal thalamic nucleus of the rat. Brain Res 595:159–163.

Levitan D, Lin JY, Wachutka J, Mukherjee N, Nelson SB, Katz DB (2019) Single and population coding of taste in the gustatory cortex of awake mice. J Neurophysiol 122:1342–1356.

Li JX, Yoshida T, Monk KJ, Katz DB (2013) Lateral hypothalamus contains two types of palatability-related taste responses with distinct dynamics. J Neurosci 33:9462–9473.

Lin JYY, Roman C, St Andre J, Reilly S, S Andre J, Reilly S (2009) Taste, olfactory and trigeminal neophobia in rats with forebrain lesions. Brain Res 1251:195–203.

Liu H, Fontanini A (2015) State dependency of chemosensory coding in the gustatory thalamus (VPMpc) of alert rats. J Neurosci 35:15479–15491.

Maier JX (2017) Single-neuron responses to intraoral delivery of odor solutions in primary olfactory and gustatory cortex. J Neurophysiol 117:1293–1304.

Maier JX, Wachowiak M, Katz DB (2012) Chemosensory convergence on primary olfactory cortex. J Neurosci 32:17037–17047.

McQueen KA, Fredericksen KE, Samuelsen CL (2020) Experience informs consummatory choices for congruent and incongruent odor-taste mixtures in rats. Chem Senses 45:371–382.

Mease RA, Metz M, Groh A (2016) Cortical sensory responses are enhanced by the higher-order thalamus. Cell Rep 14:208–215.

Meyers EM (2013) The neural decoding toolbox. Front Neuroinform 7:8.

Miller JS, Nonneman AJ, Kelly KS, Neisewander JL, Isaac WL (1986) Disruption of neophobia, conditioned odor aversion, and conditioned taste aversion in rats with hippocampal lesions. Behav Neural Biol 45:240–253.

Nakajima M, Halassa MM (2017) Thalamic control of functional cortical connectivity. Curr Opin Neurobiol 44:127–131.

Ohshiro T, Angelaki DE, Deangelis GC (2011) A normalization model of multisensory integration. Nat Neurosci 14:775–782.

Ojala M, Garriga GC (2010) Permutation tests for studying classifier performance. J Mach Learn Res 11:1833–1863.

Oyoshi T, Nishijo H, Asakura T, Takamura Y, Ono T (1996) Emotional and behavioral correlates of mediodorsal thalamic neurons during associative learning in rats. J Neurosci 16:5812–5829.

Parnaudeau S, O'Neill PK, Bolkan SS, Ward RD, Abbas AI, Roth BL, Balsam PD, Gordon JA, Kellendonk C (2013) Inhibition of mediodorsal thalamus disrupts thalamofrontal connectivity and cognition. Neuron 77:1151–1162.

Pelzer P, Horstmann H, Kuner T (2017) Ultrastructural and functional properties of a giant synapse driving the piriform cortex to mediodorsal thalamus projection. Front Synaptic Neurosci 9:3.

Piette CE, Baez-Santiago MA, Reid EE, Katz DB, Moran A (2012) Inactivation of basolateral amygdala specifically eliminates palatability-related information in cortical sensory responses. J Neurosci 32:9981–9991.

Plailly J, Howard JD, Gitelman DR, Gottfried JA (2008) Attention to odor modulates thalamocortical connectivity in the human brain. J Neurosci 28:5257–5267.

Prescott J (2012) Chemosensory learning and flavour: perception, preference and intake. Physiol Behav 107:553–559.

Prescott J (2015) Multisensory processes in flavour perception and their influence on food choice. Curr Opin Food Sci 3:47–52.

Prescott J, Johnstone V, Francis J (2004) Odor-taste interactions: effects of attentional strategies during exposure. Chem Senses 29:331–340.

Price JL, Slotnick BM (1983) Dual olfactory representation in the rat thalamus: an anatomical and electrophysiological study. J Comp Neurol 215:63–77.

Ray JP, Price JL (1992) The organization of the thalamocortical connections of the mediodorsal thalamic nucleus in the rat, related to the ventral forebrain-prefrontal cortex topography. J Comp Neurol 323:167–197.

Rebello MR, Kandukuru P, Verhagen JV (2015) Direct behavioral and neurophysiological evidence for retronasal olfaction in mice. PLoS One 10: e0117218.

Rikhye RV, Gilra A, Halassa MM (2018) Thalamic regulation of switching between cortical representations enables cognitive flexibility. Nat Neurosci 21:1753–1763.

Rousseaux M, Muller P, Gahide I, Mottin Y, Romon M (1996) Disorders of smell, taste, and food intake in a patient with a dorsomedial thalamic infarct. Stroke 27:2328–2330.

Roy DS, Zhang Y, Halassa MM, Feng G (2022) Thalamic subnetworks as units of function. Nat Neurosci 25:140–153.

Saalmann YB (2014) Intralaminar and medial thalamic influence on cortical synchrony, information transmission and cognition. Front Syst Neurosci 8:83.

Saalmann YB, Pinsk MA, Wang L, Li X, Kastner S (2012) The pulvinar regulates information transmission between cortical areas based on attention demands. Science 337:753–756.

Sadacca BF, Rothwax JT, Katz DB (2012) Sodium concentration coding gives way to evaluative coding in cortex and amygdala. J Neurosci 32:9999–10011.

Sakai N, Yamamoto T (2001) Effects of excitotoxic brain lesions on taste-mediated odor learning in the rat. Neurobiol Learn Mem 75:128–139.

Sakai N, Imada S (2003) Bilateral lesions of the insular cortex or of the prefrontal cortex block the association between taste and odor in the rat. Neurobiol Learn Mem 80:24–31.

Samuelsen CL, Fontanini A (2017) Processing of intraoral olfactory and gustatory signals in the gustatory cortex of awake rats. J Neurosci 37:244–257.

Samuelsen CL, Vincis R (2021) Cortical hub for flavor sensation in rodents. Front Syst Neurosci 15:772286.

Samuelsen CL, Gardner MPH, Fontanini A (2012) Effects of cue-triggered expectation on cortical processing of taste. Neuron 74:410–422.

Samuelsen CL, Gardner MPH, Fontanini A (2013) Thalamic contribution to cortical processing of taste and expectation. J Neurosci 33:1815–1827.

Schmitt LI, Wimmer RD, Nakajima M, Happ M, Mofakham S, Halassa MM (2017) Thalamic amplification of cortical connectivity sustains attentional control. Nature 545:219–223.

Schul R, Slotnick BM, Dudai Y (1996) Flavor and the frontal cortex. Behav Neurosci 110:760–765.

Sclafani A (2001) Psychobiology of food preferences. Int J Obes 25:S13–S16.

Scott GA, Liu MC, Tahir NB, Zabder NK, Song Y, Greba Q, Howland JG (2020) Roles of the medial prefrontal cortex, mediodorsal thalamus, and their combined circuit for performance of the odor span task in rats: analysis of memory capacity and foraging behavior. Learn Mem 27:67–77.

Sela L, Sacher Y, Serfaty C, Yeshurun Y, Soroker N, Sobel N (2009) Spared and impaired olfactory abilities after thalamic lesions. J Neurosci 29:12059–12069.

Shan G, Gerstenberger S (2017) Fisher's exact approach for post hoc analysis of a chi-squared test. PLoS One 12:e0188709.

Sherman SM (2016) Thalamus plays a central role in ongoing cortical functioning. Nat Neurosci 19:533–541.

Shi CJ, Cassell MD (1998) Cortical, thalamic, and amygdaloid connections of the anterior and posterior insular cortices. J Comp Neurol 399:440–468.

Small DM (2012) Flavor is in the brain. Physiol Behav 107:540–552.

Small DM, Veldhuizen MG, Felsted J, Mak YE, McGlone F (2008) Separable substrates for anticipatory and consummatory food chemosensation. Neuron 57:786–797.

Staubli U, Schottler F, Nejat-Bina D (1987) Role of dorsomedial thalamic nucleus and piriform cortex in processing olfactory information. Behav Brain Res 25:117–129.

Stevenson RJ, Prescott J, Boakes RA (1995) The acquisition of taste properties by odors. Learn Motiv 26:433–455.

Stroh A, Adelsberger H, Groh A, Rühlmann C, Fischer S, Schierloh A, Deisseroth K, Konnerth A (2013) Making waves: initiation and propagation of corticothalamic Ca2+ waves in vivo. Neuron 77:1136–1150.

Tham WWP, Stevenson RJ, Miller LA (2009) The functional role of the medio dorsal thalamic nucleus in olfaction. Brain Res Rev 62:109–126.

Tham WWP, Stevenson RJ, Miller LA (2011) The impact of mediodorsal thalamic lesions on olfactory attention and flavor perception. Brain Cogn 77:71–79.

Theyel BB, Llano DA, Sherman SM (2010) The corticothalamocortical circuit drives higher-order cortex in the mouse. Nat Neurosci 13:84–88.

Tong J, Mannea E, Aimé P, Pfluger PT, Yi CX, Castaneda TR, Davis HW, Ren X, Pixley S, Benoit S, Julliard K, Woods SC, Horvath TL, Sleeman MM, D'Alessio D, Obici S, Frank R, Tschöp MH (2011) Ghrelin enhances olfactory sensitivity and exploratory sniffing in rodents and humans. J Neurosci 31:5841–5846.

Veldhuizen MG, Small DM (2011) Modality-specific neural effects of selective attention to taste and odor. Chem Senses 36:747–760.

Verhagen JV, Engelen L (2006) The neurocognitive bases of human multimodal food perception: sensory integration. Neurosci Biobehav Rev 30:613–650.

Vincis R, Fontanini A (2016) Associative learning changes cross-modal representations in the gustatory cortex. Elife 5:e16420.

Yang JW, Shih HC, Shyu BC (2006) Intracortical circuits in rat anterior cingulate cortex are activated by nociceptive inputs mediated by medial thalamus. J Neurophysiol 96:3409–3422.

Yarita H, Iino M, Tanabe T, Kogure S, Takagi SF (1980) A transthalamic olfactory pathway to orbitofrontal cortex in the monkey. J Neurophysiol 43:69–85.

Yeomans MR, Mobini S, Elliman TD, Walker HC, Stevenson RJ (2006) Hedonic and sensory characteristics of odors conditioned by pairing with tastants in humans. J Exp Psychol Anim Behav Process 32:215–228.

Zhou H, Schafer RJ, Desimone R (2016) Pulvinar-cortex interactions in vision and attention. Neuron 89:209–220.